



[Handwritten Signature]
Co-ordinator
IQAC, Shri Ram College,
Muzaffarnagar

TRANSFER FUNCTION IN CHEMICAL REACTOR

¹Rishabh Bhardwaj and ¹Rajdeep Saharawat

¹Department of Basic Science

Shri Ram College, Muzaffarnagar

Email for correspondence (bhardwairs14@gmail.com)

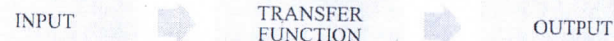
ABSTRACT

Transfer functions have been found to successfully identify properties of a chromatographic system where they have been empirically determined via Bode plots of pulse test experiments. In the frequency domain, there is a linear relationship between the time delay analogue of the system and the packing height of the column. Breaking down a transfer function into classical chromatographic principles also holds potential for the further identification of chromatography.

Keywords: domain, function, systems, flow

INTRODUCTION

A control system has two most important things one is output signal and other is input signal. The relationship between output signal and input signal is known as transfer function. This relationship of input and output signal can be represented by block diagram which has arrows towards the transfer function for input and arrows going away from transfer function for output. If we give some input or disturbance to the system then the output is influenced by this input signal and their relationship between the cause and effect is related by transfer function.



R(s) is Laplace Transform of input signal and C(s) is Laplace Transform for output signal, so transfer function G(s) is given as

$$G(s) = \frac{C(s)}{R(s)} \implies R(s) \cdot G(s) = C(s)$$

So, output of a system can be represented as product of transfer function and laplace transform of input signal.

Why input, output and other signals are represented in Laplace form in a control system?

Input and output of a control system may or may not be in same domain, they can be in different parameters. Like in HPLC input is a pulse flow rate but observed output is disturbance in the level and the concentration which are time function. So, input and output are totally in different domain in HPLC, so to compare or to relate this input and out we transformed them and for that we use a mathematical trick which is laplace transform. We can transform all kind of input and output signals to their laplace transform. Laplace transform is simply given by dividing output laplace transfer function to input laplace transfer function.



Where, $R(s) = \mathcal{L}\{r(t)\}$, $C(s) = \mathcal{L}\{c(t)\}$ & $G(s) = \frac{\mathcal{L}\{c(t)\}}{\mathcal{L}\{r(t)\}}$

[Handwritten Signature]
Chairman
IQAC, Shri Ram College,
Muzaffarnagar
Page 59

Where, $r(t)$ and $c(t)$ are time domain function of input and output signal respectively.

DEFINITION OF TRANSFER FUNCTION

The transfer function of a control system is defined as the ration of the Laplace transform of the output variable to Laplace transform of the input variable.

$$G(s) = \frac{C(s)}{R(s)}$$

LIQUID LEVEL

In (Figure1), we have a tank of uniform cross-sectional area A , flow resistance R for valve and let q_0 be the volumetric flow rate (volume/time). There for their relation between the head h , flow resistance R and volumetric flow rate q_0 , given as

$$q_0 = \frac{h}{R}$$

Let q volumetric flow rate of liquid of constant density ρ enters the tank. To analyze this system, we have to find transfer function and to do so we apply a mass balance around the tank:

$$(\text{Rate of mass flow in}) - (\text{Rate of mass flow out}) = (\text{Rate of accumulation of mass in tank})$$

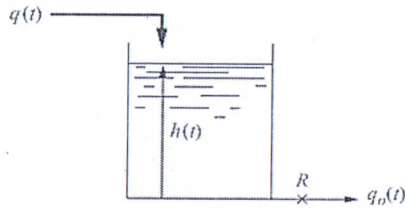


Figure 1: liquid level tank

In terms of the variables used in this analysis, the mass balance becomes

$$\rho q(t) - \rho q_0(t) = \frac{d(\rho Ah)}{dt}$$

$$q(t) - q_0(t) = A \frac{dh}{dt}$$

Combining above Equations to eliminate $q_0(t)$ gives the following linear differential equation:

$$q - \frac{h}{R} = A \frac{dh}{dt}$$

We will introduce deviation variables into the analysis before proceeding to the transfer function. Initially, the process is operating at steady state, which means that $dh/dt = 0$ and we get

$$q_s - \frac{h_s}{R} = 0$$

where the subscript s has been used to indicate the steady-state value of the variable. Subtracting

$$q - q_s = \frac{1}{R} (h - h_s) + A \frac{d(h - h_s)}{dt}$$

If we define the deviation variables as

$$Q = q - q_s$$

$$H = h - h_s$$

then Equation can be written

$$Q = \frac{1}{R} H + A \frac{dH}{dt}$$

Taking the transform of Equation gives

IQAC, Shri Ram College, Muzaffarnagar

$$Q(s) = \frac{1}{R} H(s) + AsH(s)$$

Notice that $H(0)$ is zero, and therefore the transform of dH/dt is simply $sH(s)$. Equation can be rearranged into the standard form of the first-order lag to give

$$\frac{H(s)}{Q(s)} = \frac{R}{\tau s + 1}$$

Where $\tau = AR$. To the determination of the steady-state value of H when the flow rate $Q(t)$ changes according to a unit-step change; thus

$$Q(t) = u(t)$$

Where $u(t)$ is the symbol for the unit-step change. The transform of $Q(t)$ is

$$Q(s) = \frac{1}{s}$$

Combining we get

$$H(s) = \frac{1}{s} \frac{R}{\tau s + 1}$$

Applying the Inverse Laplace to $H(s)$ gives

$$H(t) = R + e^{-\frac{t}{\tau}}$$

As t tends to infinity we can see that the ultimate change in $H(t)$ for unit step change in input $Q(t)$ is given as R . We have calculated the transfer function for a physical example of a first order system. We will see more examples of first-order systems.

NON-INTERACTING SYSTEMS AND INTERACTING SYSTEMS

Usually a process chemist in an industry has to deal with several first order process which are connected together. To show this we have possible arrangements of the tank shown in figure 2 and figure 5. the outlet from the tank 1 discharge directly into atmosphere before splitting into tank 2 and flow from R_1 depends only on h_1 . The change in height h_2 of tank 2 has no affect on the tank 1. This type of system is known as non-interacting system. Where as in figure 5 the flow through R_1 will be dependent on the difference of h_1 and h_2 . It means flow will be influenced by both the tank height, this type of system is called interacting systems.

NON-INTERACTING SYSTEM

In earlier example of liquid- level, we have constant density of liquid, uniform cross-sectional area and linear flow resistance. The main objective was to find transfer function that relates h_2 to q , that is, $H_2(s)/Q(s)$. For this we will find transfer function for each tank, $Q_1(s)/Q(s)$ and $H_2(s)/Q_1(s)$, by writing a mass balance around each tank and then eliminate the intermediate flow $Q_1(s)$ and produce the desired transfer function. A balance on tank 1 gives

$$q - q_1 = A_1 \frac{dh_1}{dt}$$

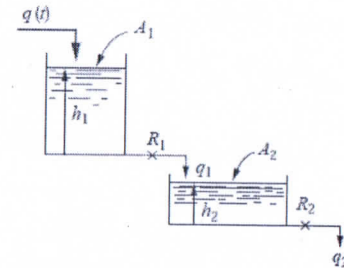


Figure-2 Two tank liquid level system: Non-interacting

A balance on tank 2 gives

$$q_1 - q_2 = A_2 \frac{dh_2}{dt}$$

The flow-head relationships for the two linear resistances are given by the expressions

$$q_1 = \frac{h_1}{R_1}$$

$$q_2 = \frac{h_2}{R_2}$$

Combining Equation same manner as done in liquid level and introducing deviation variables give the transfer function for tank 1

$$\frac{Q_1(s)}{Q(s)} = \frac{1}{\tau_1 s + 1}$$

Where $Q_1 = q_1 - q_{1s}$, $Q = q - q_s$, and $\tau_1 = R_1 A_1$.

In the same manner, we can combine Equations to obtain the transfer function for tank 2

$$\frac{H_2(s)}{Q_1(s)} = \frac{R_2}{\tau_2 s + 1}$$

Where $H_2 = h_2 - h_{2s}$ and $\tau_2 = R_2 A_2$.

Having the transfer function for each tank, we can obtain the overall transfer function $H_2(s)/Q(s)$ by multiplying Equations to eliminate $Q_1(s)$:

$$\frac{H_2(s)}{Q(s)} = \frac{1}{\tau_1 s + 1} \frac{R_2}{\tau_2 s + 1}$$

Notice that the overall transfer function is the product of two first-order transfer functions, each of which is the transfer function of a single tank operating independently of the other.

For a unit step change in Q , we obtain

$$H_2(s) = \frac{1}{s} \frac{R_2}{(\tau_1 s + 1)(\tau_2 s + 1)}$$

Inversion by means of partial reaction expansion gives

$$H_2(t) = R_2 \left[1 - \frac{\tau_1 \tau_2}{\tau_1 - \tau_2} \left(\frac{1}{\tau_2} e^{-t/\tau_1} - \frac{1}{\tau_1} e^{-t/\tau_2} \right) \right]$$

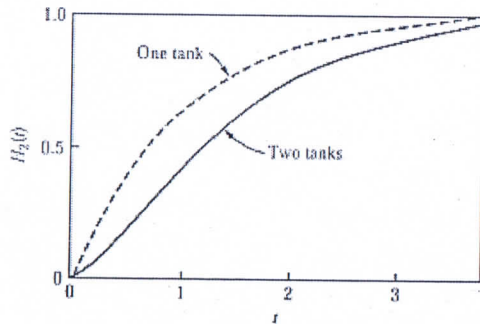


Figure-3 variation of height of tank-2 with respect to time

We can generalize the result for Several Non-interacting systems in series i.e. overall transfer function is nothing but the product of individual transfer functions. So, the block representation of several non-interacting system is given as:

Co-ordinator

IQAC, Shri Ram College,
Muzaffarnagar



The block diagram is equivalent to the relationships

$$\frac{X_1(s)}{X_0(s)} = \frac{k_1}{\tau_1 s + 1}$$

$$\frac{X_2(s)}{X_1(s)} = \frac{k_2}{\tau_2 s + 1}$$

etc.

$$\frac{X_n(s)}{X_{n-1}(s)} = \frac{k_n}{\tau_n s + 1}$$

To obtain the overall transfer function, we simply multiply the individual transfer functions; thus

$$\frac{X_n(s)}{X_0(s)} = \prod_{i=1}^n \frac{k_i}{\tau_i s + 1}$$

To show how the transfer lag is increased as the number of stages increases, the unit-step response curves for several systems containing one or more first order stages in series.

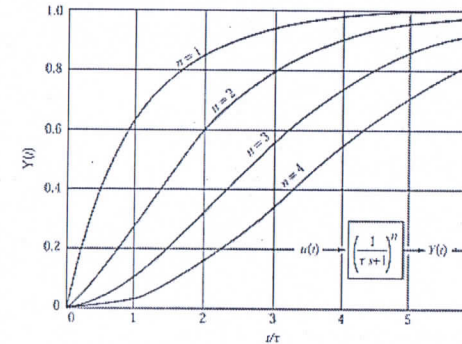


Figure-4 variation of height of n tanks with respect to time

INTERACTING SYSTEM

In figure (b) interacting system, we will derive the transfer function similarly as it was done for non-interacting system. The analysis is started by writing mass balances on the tanks. The balances on tanks 1 and 2 are the same as before and are given by Equations

$$\text{Tank 1} \quad q - q_1 = A_1 \frac{dh_1}{dt}$$

$$\text{Tank 2} \quad q_1 - q_2 = A_2 \frac{dh_2}{dt}$$

Chairman
IQAC, Shri Ram College,
Muzaffarnagar

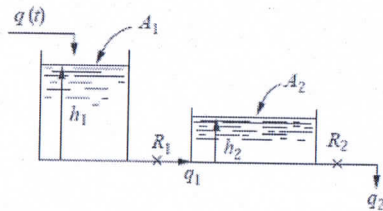


Figure-5 Two tank liquid level system: interacting

However, the flow-head relationship for R₁ is now

$$q_1 = \frac{(h_1 - h_2)}{R_1}$$

The flow-head relationship for R₂ is the same as before

$$q_2 = \frac{h_2}{R_2}$$

A simple way to combine Equations is to first express them in terms of deviation variables, transform the resulting equations, and then combine the transformed equations to eliminate the unwanted variables. At steady state, Equations can be written

$$q_s - q_{1s} = 0$$

$$q_{1s} - q_{2s} = 0$$

Subtracting Equations and introducing deviation variables give

Tank 1 $Q - Q_1 = A_1 \frac{dh_1}{dt}$

Tank 2 $Q_1 - Q_2 = A_2 \frac{dh_2}{dt}$

Expressing Equations in terms of deviation variables gives

Valve 1 $Q_1 = \frac{h_1 - h_2}{R_1}$

Valve 2 $Q_2 = \frac{h_2}{R_2}$

Transforming Equations Gives

Tank 1 $Q(s) - Q_1(s) = A_1 s H_1(s)$

Tank 2 $Q_1(s) - Q_2(s) = A_2 s H_2(s)$

Valve 1 $R_1 Q_1(s) = H_1(s) - H_2(s)$

Valve 2 $R_2 Q_2(s) = H_2(s)$

We have four algebraic equations containing five unknowns: Q, Q₁, Q₂, H₁, and H₂. These equations may be combined to eliminate Q₁, Q₂, and H₁ and to arrive at the desired transfer function:

$$\frac{H_2(s)}{Q(s)} = \frac{R_2}{\tau_1 \tau_2 s^2 + (\tau_1 + \tau_2 + A_1 R_2) s + 1}$$

If the tanks are non-interacting, the transfer function relating inlet flow to outlet flow is (assuming that $\tau_1 = \tau_2$)

$$\frac{Q_2(s)}{Q(s)} = \left(\frac{1}{\tau s + 1} \right)^2$$

The unit-step response for this transfer function can be obtained by the usual procedure to give

$$Q_2(t) = 1 - e^{-t/\tau} - \frac{t}{\tau} e^{-t/\tau}$$

If the tanks are interacting, the overall transfer function, is (assuming that $A_1 = A_2$)

$$\frac{Q_2(s)}{Q(s)} = \frac{1}{\tau^2 s^2 + 3\tau s + 1}$$

By application of the quadratic formula, the denominator of transfer function can be written as

$$\frac{Q_2(s)}{Q(s)} = \frac{1}{(0.383\tau s + 1)(2.62\tau s + 1)}$$

For this example, we see that the effect of interaction has been to change the effective time constants of the interacting system. One-time constant has become considerably larger and the other smaller than the time constant τ of either tank in the non-interacting system. The response of Q₂(t) to a unit-step change in Q(t) for the interacting case is

$$Q_2(t) = 1 + 0.17e^{-t/0.38\tau} - 1.17e^{-t/2.62\tau}$$

In below Figure the unit-step responses for the two cases are plotted to show the effect of interaction. From this figure, it can be seen that interaction slows up the response. This result can be understood on physical grounds in the following way: If the same size step change is introduced into the two systems, the flow from tank 1 (q₁) for the non-interacting case will not be reduced by the increase in level in tank 2. However, for the interacting case, the flow q₁ will be reduced by the buildup of level in tank 2. At any time t₁ following the introduction of the step input, q₁ for the interacting case will be less than for the non-interacting case with the result that h₂ (or q₂) will increase at a slower rate.

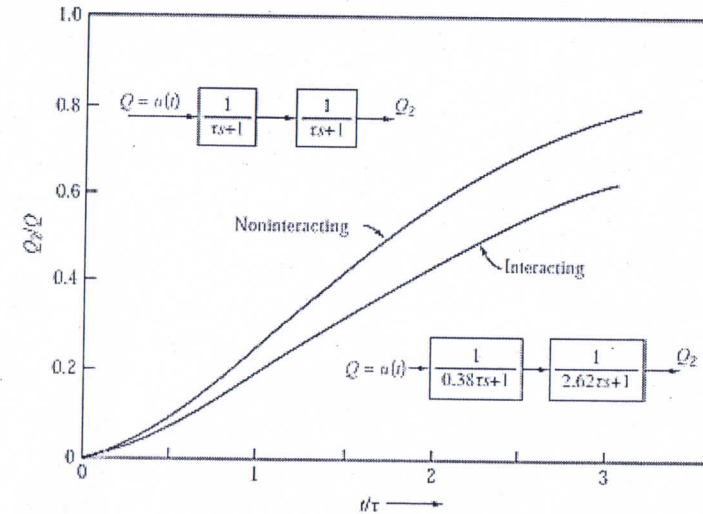


Figure-6 Effect of interaction on step response of two tank system

In general, the effect of interaction on a system containing two first-order lags is to change the ratio of effective time constants in the interacting system. In terms of the transient response, this means that the interacting system is more sluggish than the non-interacting system.

SUMMARY

We discussed the response of first-order systems in series. We observed that the nature of the response is dependent upon whether the first-order systems in series form a non-interacting or an interacting system. We analyze the response of these two different types of systems and study their behavior and found that interacting system is more sluggish than non-interacting system.

Co-ordinator
IQAC
Muzaffarnagar

Chairman
IQAC, Shri Ram College
Muzaffarnagar

ADVANTAGES OF TRANSFER FUNCTION


1. Transfer function is a mathematical model and it gives the gain of the system.
2. Since laplace transform is used, the terms are simple algebraic expressions and differential terms are not present.
3. If the transfer function of a system is known, the response of the system to any input can be determined very easily.
4. Transfer function helps in the study of stability analysis of the system.

REFERENCES:

Y. Christy, D. Dinesh Kumar, Modelling and Design of Controllers for Interacting Two Tank Hybrid System, *International Journal of Engineering and Innovative Technology* **2014**, 3, 88-91.
 L.Thillai Rani, N. Deepa, A. Arulselvi, Modelling and Intelligent Control of two Tank Interacting Level Process, *International Journal or Recent Technology and Engineering* **2014**, 3, 30-36.
 S. Saju, B.R. Revathi, K. Parkavi, Suganya, Modelling and Control of Liquid Level Nonlinear Interacting and Non-Interacting System, *International Journal of Advanced Research in Electrical, Electronics and Instrumentation Engineering*. **2014**, 3, 66-71
 D.Hariharan, S. Vijayachitra, Modelling and Real Time Control of Two Conical Tank Systems of Non-interacting and Interacting type, *International Journal of Advanced Research in Electrical, Electronics and Instrumentation Engineering*, **2013**, 2, 5728-5733
 Mathematical Modeling of Interacting and Non-Interacting Tank System Mr. Parvatl. B.J., Mr. Deo.S.A. and Mr. Kadu C.B, *International Journal of Application or Innovation in Engineering*. **2015** 4, 86-92
 Vinay Kumar, Rekha Jha, Liquid Level Control of Multi Tank System And Their Performance Analysis, *International Journal of Scientific Research And Education*, **2015** 35, 3377-3385,



Co-ordinator
IQAC, Shri Ram College,
Muzaffarnagar

ISARA INSTITUTE OF MANAGEMENT & PROFESSIONAL STUDIES




WWW.IIMPS.IN

EARN YOUR MBA



Accreditation & Ranking




UGC / NCTE Approved.

INFO@IIMPS.IN
 011-41005174

RESEARCH GATEWAY


STOP PLAGIARISM



- 1 Submit your content in Word File.
- 2 Get report in 48 hrs.
- 3 Matching content or references will be fixed.
- 4 Citation for your work.
- 5 Get accurate user friendly report.

researchgateway.in | info@researchgateway.in | +91 820578729


Arogyam Ayurveda
 Holistic Healing through herbs



AROGYAM ONLINE


PARIVARTAN PSYCHOLOGY CENTER

**COLOR PSYCHOLOGY :
 HOW COLOR AFFECT YOUR CHILD**



BLUE	Calm your Child's Mind & Body
YELLOW	Enhances Cognitive skills Stimulates the Memory
PINK	Evokes Empathy, makes your Child Calm
RED	Excites and energizes your Child's Body
GREEN	Enhances Reading span and Comprehension

www.parivartan4u.com



Confuse about your child or future?

Chairman
IQAC, Shri Ram College,
Muzaffarnagar

भारतीय भाषा, शिक्षा, साहित्य एवं शोध

ISSN 2321 – 9726
WWW.BHARTIYASHODH.COM



INTERNATIONAL RESEARCH JOURNAL OF
MANAGEMENT SCIENCE & TECHNOLOGY

ISSN – 2250 – 1959 (0) 2348 – 9367 (P)
WWW.IRJMS.T.COM



INTERNATIONAL RESEARCH JOURNAL OF
COMMERCE, ARTS AND SCIENCE

ISSN 2319 – 9202
WWW.CASIR.I.COM



INTERNATIONAL RESEARCH JOURNAL OF
MANAGEMENT SOCIOLOGY & HUMANITIES

ISSN 2277 – 9809 (0) 2348 - 9359 (P)
WWW.IRJMSH.COM



INTERNATIONAL RESEARCH JOURNAL OF SCIENCE
ENGINEERING AND TECHNOLOGY

ISSN 2454-3195 (online)

WWW.RJSET.COM



INTEGRATED RESEARCH JOURNAL OF
MANAGEMENT, SCIENCE AND INNOVATION

ISSN 2582-5445

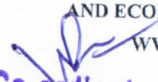
WWW.IRJMSI.COM



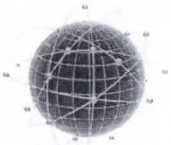
JOURNAL OF LEGAL STUDIES, POLITICS
AND ECONOMICS RESEARCH

WWW.JLPER.COM

JLPE


Co-ordinator
IQAC, Shri Ram College,
Muzaffarnagar


Chairman
IQAC, Shri Ram College,
Muzaffarnagar



IOSR Journals

International Organization
of Scientific Research

*International Organization
of Scientific Research
Community of Researchers*

Is hereby honoring this certificate to

Dr Manoj Kumar Mittal

In recognition of the Publication of Manuscript entitled
*A Comparative Review analysis of Various Materials for Solid
Oxide Fuel Cells*

Published in IOSR Journal of Applied Physics

Volume 13, Issue 2, Ser. IV, Mar. – Apr. 2021


Co-ordinator
IQAC, Shri Ram College,
Muzaffarnagar

Impact Factor : 3.15

E-mail id : jap@iosrmail.org

Web.: www.iosrjournals.org

IOSR-JAP is peer reviewed refereed journal approved by UGC


Chairman
IQAC, Shri Ram College,
Muzaffarnagar



Editor in Chief
IOSR-JAP

A Comparative Review analysis of Various Materials for Solid Oxide Fuel Cells

Dr Manoj Kumar Mittal

Associate Professor, Shri Ram College, Muzaffar Nagar

Abstract

Solid State Oxide Fuel Cells (SOFC) offer clean and efficient power generation systems with good fuel flexibility, high power density, low pollution, modularity and high energy conversion efficiency. The conventional SOFCs operate at a higher temperature of about 1000 °C. This limits the use of materials to be used for their construction. Presently, the major research effort ongoing is to develop the low cost intermediate temperature (IT) SOFC. These cells work in the temperature range of 500–800 °C with power densities as high as possible. The main difficulty in developing these SOFCs is the degrading performance of fuel cells owing to lower ion conduction of the electrolyte. The selection of materials for different cell components is based on sufficient chemical and structural stability at intermediate temperatures, suitable electrical-conducting properties for various cell functions, minimal reactivity among cell components and matching thermal expansion of various components. In this review, comparative study of component materials of SOFC, effect of processing on properties of SOFC and various designs of SOFC have been compared.

Keywords: SOFC, anode, cathode, electrolyte, interconnect

I. Introduction

Solid state oxide fuel cell (SOFC) technology has made significant progress in the recent years. It promises to revolutionize electric power generation in the 21st century. The biggest advantages of SOFC are high efficiency and environmental friendliness [1]. SOFCs have several additional advantages over conventional power generation systems some of which include high power density, fuel flexibility, modularity, low emissions of CO₂, NO_x, CO, SO₂, etc. [2–4]. SOFCs have been developed as a practical high temperature fuel cell technology. Since there is no liquid electrolyte, therefore corrosion of its supporting materials is prevented which reduces the problem related to the electrolyte management [5].

The operating temperature of solid oxide fuel cells is above 900 °C. Because of the high temperature operation, the exhaust heat is of good quality. The multidimensional applications like space heating, household hot water and process steam utilize the waste heat produced, during the operation of solid oxide fuel cells [13].

At the high working temperature of SOFC, the fuel cell operating environments affect the chemical stability of its cell components which may lead to corrosion of components and undesirable phase formation at interfaces between different cell components (electrolyte, anode, cathode and interconnect). To solve these problems, the working temperature of SOFC should be lowered to around 700–800 °C as reported by Badwal *et al.* [6]. If the working temperatures of SOFCs are lowered, it would lead to the development of its thermal stability and reduce startup time. As a result, they can be used as auxiliary power units for automobiles [2, 10, 16]. Many studies aim at reducing SOFC operating temperatures. But the lowering of the operation temperature leads to reduction in the ionic conduction of the electrolyte and hence the power density. To solve these problems, alternate low cost component materials and designs need to be broadly explored that remain stable and durable even at these temperatures [22].

SOFC COMPONENTS AND ITS DESIGNS

The single solid oxide fuel cell basically comprises anode, cathode, an electrolyte, interconnects and sealing materials in the solid state [6]. The ceramic oxide electrolyte shows conduction at high temperature of about 1000 °C. Figure 1 shows the working principle of SOFC. The fuel is fed to the anode where it undergoes an oxidation reaction. The electrons so released move to the external circuit. Oxygen ions are formed due to reduction at the cathode. The flow of electrons in the external circuit from the anode to the cathode leads to the production of electricity [43].

SOFC can be designed as (a) planar (b) tubular and (c) monolithic. In terms of stack design, planar and tubular designs are more popular. The planar SOFC may be in the form of a circular disk or in a square shape.

Manoj Kumar Mittal
 IQAC, Shri Ram College,
 Muzaffarnagar

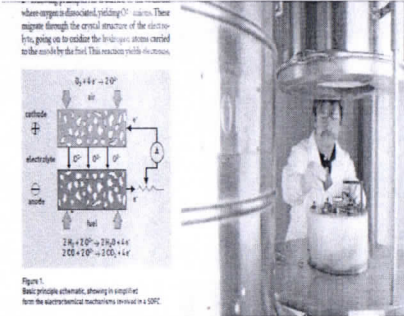


Fig. 1: Working Principle of SOFC.

The fuel is fed from the central axis in the case of circular disk or from the edges if it is of a square shape. The tubular SOFC may have varying diameter: a large diameter (> 15 mm), or much smaller diameter (< 5 mm). Figure 2a illustrates typical tubular cell bundle and Figure 2b planar cell stacks.

One of the inbuilt advantages of tubular SOFC is that the air and the fuel are naturally isolated as one end of the tube is closed; therefore, no seal is required. However, in the case of planar cell stacks, there must be a provision of a seal for the isolation of fuel and air.

Due to no seal requirement for the tubular cells, they may perform well for several years. Nevertheless, they lag behind the planar cells in respect of lower volume power density, and higher manufacturing cost [11].

Large tubular SOFC design

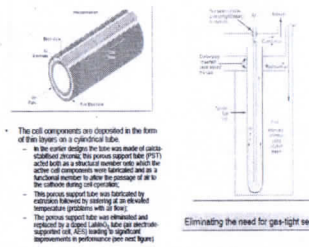


Fig. 2a: Tubular SOFC.

Manoj Kumar Mittal
 Chairman
 IQAC, Shri Ram College,
 Muzaffarnagar

Cell and stack designs

• Planar SOFC design

– Cell components are configured as flat plates which are connected in electrical series:

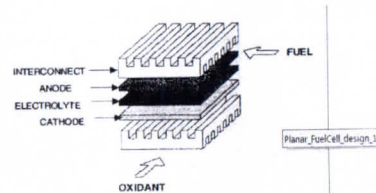


Fig. 2b: Planar SOFC.

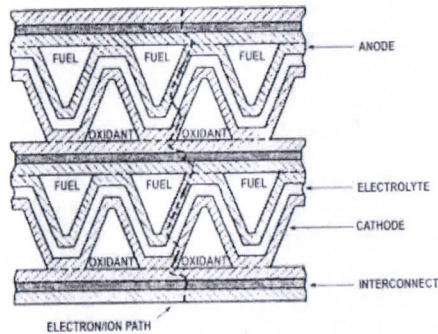


Fig. 2c: Monolithic SOFC.

A monolithic design of SOFC was first suggested in the early 1980s at Argonne National Laboratory (ANL) [26]. In this design, various components of the cell are fabricated in the form of thin layers. In the co-flow version, the cell resembles an array of adjoining fuel and oxidant channels, looking like a honeycomb. There are two types of laminated structures in a cell:

- Anode/Electrolyte/Cathode
- Anode/Interconnect/Cathode

Anode/Electrolyte/Cathode composite is uneven and is stacked alternately between flat Anode/Interconnect/Cathode (Figure 2c). While the monolithic SOFCs present the highest power density out of all the possible SOFC designs, their fabrication has proven to be a matter of concern because it deals with co-sintering of the cell components at high temperatures [12].

SOFC MATERIALS – A COMPARATIVE STUDY

By the end of 19th century, Zirconia with Yttria in solid solution (YSZ) was identified by Nernst [37]. It was used as an electrolyte in an SOFC in 1937 by Baur and Preis [38]. As high temperature was a compulsion for

successful performance of this electrolyte, a conducting oxide as cathode in contact with air was demanded. A cobalt perovskite was reported in 1966 [39], and the well-known lanthanum–strontium manganite (LSM) was introduced in the 1970s [40]. A composite of nickel and electrolyte material as anode was introduced in 1964 [41]. After a detailed study of candidate materials, Siemens Westinghouse adopted this set of materials in 1980s for the tubular cell configuration [42] and thereby proved to be a standard [28]. Table 1 shows the comparison of cell component technology for tubular SOFCs:

Table 1: Evolution of Fuel Cell Technology for SOFCs [44].

Comp-onent	Ca. 1965	Ca. 1975	Ca. 1998 ^a	At present
Anode	• Porous Pt	• Ni/ZrO ₂ cermet ^b	<ul style="list-style-type: none"> • Ni/ZrO₂ cermet^b • Deposit slurry, EVD fixed^d • 12.5 × 10⁻⁶ cm/cm °C CTE • ~150 μm thickness • 20 to 40% porosity 	<ul style="list-style-type: none"> • Copper cermet anodes • LSCFO-GDC • LSCM • LST
Cathode	• Porous Pt	• Stabilized ZrO ₂ impregnated with praseodymium oxide and covered with SnO doped In ₂ O ₃	<ul style="list-style-type: none"> • Doped lanthanum magnate • Extrusion, sintering • ~2 mm thickness • 11 × 10⁻⁶ cm/cm °C CTE from room temperature to 1000 °C • 30 to 40% porosity 	<ul style="list-style-type: none"> • LSCF • Sm_{0.5}Sr_{0.5}CoO₃ • Lanthanum cobalites
Electrolyte	• Yttria stabilized ZrO ₂ 0.5 mm thickness	• Yttria stabilized ZrO ₂	<ul style="list-style-type: none"> • Yttria stabilized ZrO₂ (8 mol% Y₂O₃) • EVD^d • 10.5 × 10⁻⁶ cm/cm °C CTE from room temperature to 1000 °C • 30 to 40 μm thickness 	<ul style="list-style-type: none"> • ZrO₂ – Y₂O₃ • LSGM • SNDC
Interconnect	• Pt	• Mn doped cobalt cromite	<ul style="list-style-type: none"> • Doped lanthanum chromite • Plasma spray • 10 × 10⁻⁶ cm/cm °C CTE 	<ul style="list-style-type: none"> • Cermet • Ferritic steels

a – Specification for Siemens Westinghouse SOFC; b – Y₂O₃ stabilized ZrO₂

c – “Fixed EVD” means additional ZrO₂ is grown by EVD to fix (attach) the nickel anode to the electrolyte. This process is expected to be replaced; d – EVD = electrochemical vapor deposition.

Cathode

The cathode is an electrode of SOFC where electrochemical reduction of oxygen takes place. The basic requirement for cathode can be summarized as:

- Comparatively simple fabrication method and low cost;
- Sufficient porosity to allow the diffusion of oxygen and high catalytic activity to facilitate oxygen reduction;
- Chemical compatibility with other cell components under working conditions;
- Matching thermal expansion coefficients (TEC) and large triple phase boundary (TPB);
- High electronic and ionic conductivity [4, 12, 13].

Ralph *et al.* reported that at high temperatures, LSM proves to be the best option as cathode material for YSZ based SOFCs. At low temperatures, LSF and layered structured material YBaCuO are the reasonable cathode materials for YSZ based SOFCs. For Ceria based electrolytes, Gd_{0.5}Sr_{0.2}CoO₃ is the best candidate at low temperature. Also BSCaCuO was tried for the first time showing better areal resistance and low activation energy [26].

MvEvoy *et al.* mentioned that mixed conductors like lanthanum strontium cobaltite are preferred to LSM due to the formation of an insulating interphase of lanthanum Zirconate [28]. Badwal *et al.* reported that Co or Ni may replace Mn providing faster kinetics at low temperatures for zirconia based electrolytes in spite of strong reactivity. LaSrCoO₃ or LaSrCoFeO₃ electrodes and the intermediate phase formation by thin layers of doped ceria prove to be promising options for Ce based electrolytes [6]. Haile *et al.* emphasized the search for transition metal perovskites in order to replace LSM at high temperatures like lanthanum cobalites but they are also found unsuitable for YSZ based SOFCs at elevated temperatures. Recently, LSCF and Sm_{0.5}Sr_{0.5}CoO₃ have emerged as reasonable cathode candidates at low temperatures [33]. Singhal *et al.* showed that doped lanthanum manganite satisfies good qualities of a cathode at elevated temperatures. At lower temperatures, polarization losses pose a great problem towards cathode stability. So, the concept of composite cathode was introduced [11]. Taroco *et al.* recently mentioned that the choice of electrolyte decides the choice of cathode. The concentration of dopants also affects the electronic conductivity as well as TEC of the materials. Doping with Sr on the A-site and with Fe and Co on the B-site in the perovskite increases both the ionic and electronic conductivities [29]. Also LSCF cathodes are fairly compatible with GDC electrolyte [3].

Electrolyte Materials

The electrolyte is the part of the cell allowing the conduction of ions between the cathode and anode. The basic performance requirements are [4, 12]:

- The oxide-ion conductivity should be more than 10^{-2} Scm^{-1} at the working temperature and minimum electronic conduction;
- High density so that the gas impermeability is promoted;
- Oxygen partial pressure and thermodynamically stable over a long range of temperature and moderate cost;
- TEC matching with cell components and the concept of thin layers (less than 30 μm);
- For fracture resistance greater than 400 MPa, mechanical properties should be appropriate at room temperature;

The most explored and developed electrolytes have been the zirconia based ceramic materials at the elevated temperatures [3]. According to Bujalski *et al.*, zirconia doped with 8 to 10 mole% Ytria (YSZ) is still the most effective electrolyte for the high temperature SOFC as zirconia is highly stable in both the reducing and oxidizing environments that are experienced at the anode and cathode, respectively and the ionic conductivity of YSZ (0.02 Scm^{-1} at 800 °C and 0.1 Scm^{-1} at 1000 °C) is comparable with that of liquid electrolytes and it can be made very thin (25–50 μm) ensuring that the ohmic loss in the SOFC is comparable with other fuel cell types. Many other electrolytes such as Bi_2O_3 , CeO_2 and Ta_2O_5 have also been investigated with mixed success at high temperatures [31].

Badwal *et al.* mentioned that the materials typically used in SOFC include zirconia, ceria and perovskite like lanthanum gallate doped at both A and B sites. These perovskites are prone to changes in their stoichiometry due to which many impurity phases like $\text{La}_2\text{Zr}_2\text{O}_7$ and SrZrO_3 are formed. To eliminate this, thin layers of doped ceria are proposed to be introduced between Zr based electrolytes and $\text{La}(\text{Co}, \text{Fe})\text{O}_3$. But the contact needs low temperature operation for better performance of the cell [6]. Taroco *et al.* reported that doped CeO_2 and doped lanthanum gallate are two candidates in intermediate temperature SOFCs (600–800 °C). Doped ceria offers ionic conductivities about one order of magnitude greater than stabilized zirconia under similar temperature conditions. The $\text{Ce}_{0.9}\text{Gd}_{0.1}\text{O}_{1.95}$ (CGO) composition is reliable for IT-SOFC applications more as it has high ionic conductivity at 500 °C. In case of gadolinium doped ceria (GDC), at elevated temperatures, Ce^{4+} converts to Ce^{3+} under the reducing anode atmosphere. This leads to faster consumption of fuel leading to deteriorating cell performance [14, 17]. To avoid the problem, a thin film of YSZ between the Ce electrolyte and the anode is inserted [9, 20]. The electronic conductivity is lower at less temperatures around 500 °C and it has been concluded that this temperature could be an optimal one for ceria based fuel cells [21].

The compositions like $\text{La}_{1-x}\text{Sr}_x\text{Ga}_{1-y}\text{Mg}_y\text{O}_{3-\delta}$ (LSGM) have presented high ionic conductivities in oxidizing and reducing atmospheres [3]. But such ceramics show instability under reducing atmospheres and also Ga losses are experienced, thereby leading to new phases formation [21, 30]. These reasons limit the use of doped lanthanum gallate to be used as electrolyte in SOFC.

The comparison of various electrolyte materials has been depicted in Table 2 in terms of their ionic conductivities and thermal expansion coefficients:

Table 2: Ionic Conductivity and TEC of Suggested Electrolyte Materials in Air at 800 °C [29].

Composition	σ_i at 800 °C (Scm^{-1})	TEC ($\times 10^{-6} \text{ K}^{-1}$)
$(\text{Y}_2\text{O}_3)_{0.08}(\text{ZrO}_2)_{0.92}$	10.5	0.03
$(\text{Sc}_2\text{O}_3)_{0.08}(\text{ZrO}_2)_{0.92}$	10.7	0.13
$\text{Ce}_{0.9}\text{Gd}_{0.1}\text{O}_{1.9}$	12.5	0.053
$\text{Ce}_{0.9}\text{Sm}_{0.1}\text{O}_{1.9}$	12.2	0.095
$\text{La}_{0.9}\text{Sr}_{0.1}\text{Ga}_{0.9}\text{Mg}_{0.1}\text{O}_{2.85}$	10.7	0.1

Other options for use in IT-SOFC are salt-oxide composites and NANOCOFC materials (nanocomposites for advanced fuel cell technology) [17, 18]. Ralph *et al.* investigated the high temperature ceramic electrolyte material, Bi_2O_3 which has the highest ionic conductivity because its crystal structure is quite spacious. All the bismuth based electrolytes have the problem that Bi^{3+} reduces to Bi metal that proves fatal to the electrolyte at high oxygen partial pressures [32]. The stability of low temperature candidate LSGM with some fuels is yet unknown. So, YSZ proves to be the best electrolyte material at high temperatures, but at low temperatures, doped ceria remains the only option [26]. Steele *et al.* reported that the specific conductivity of a solid electrolyte varies as the reciprocal of temperature, e.g., the attainment of target value of ionic conductivity of YSZ at about 700 °C predicts its suitability to be used as a promising material at high temperatures, whereas

CGO attains the same at about 500 °C that makes it suitable to be used at low temperatures successfully. They added that when the thin electrolyte films are used, the operating temperature of SOFC may be lowered [5]. Singhal *et al.* concluded that to make the stabilized zirconia operational in the low temperature regime, either the thickness of YSZ electrolyte may be decreased or Y may be replaced with other acceptors, e.g., scandia doping, but the high cost of scandium puts a question mark. Also at high temperatures above about 600 °C, ceria based electrolytes possess electronic conductivity which may deteriorate the performance of the cell because of problems associated with the PEN (positive electrode-electrolyte-negative electrolyte) structure [14].

These problems are solved at low temperatures successfully. They also listed some of the drawbacks of LSGM as an electrolyte, viz., its stability and the cost of constituents. Even then LSGM is being used as a promising electrolyte at Mitsubishi Materials Corporation, Japan [11]. Haile *et al.* raised a question on the long term feasibility of ceria based SOFCs because of its high electronic conductivity though it has good ion transport properties, and the internal stress resulting from the chemical expansion of ceria during reduction processes. They added that LSGM is restricted to a temperature range of about 700–1000 °C. To avoid the reactivity of lanthanum gallate with nickel, the buffer layers of ceria have been used between the anode and the electrolyte [33]. Chao *et al.* reported that to develop IT-SOFC, either alternate materials having higher ionic conductivity like LSGM having maximum power density of 0.612 W/cm^2 at 500 °C and $\text{Sm}_{0.075}\text{Nd}_{0.075}\text{Ce}_{0.85}\text{O}_{2-\delta}$ (SND) having the maximum power density 0.32 W/cm^2 at 500 °C [27] but less stable as compared to Ytria-stabilized zirconia (YSZ) or to reduce electrolyte thickness so as to improve the fuel cell performance at low temperatures [22].

They also designed a corrugated membrane of thin film electrolyte by using the technique of nanosphere lithography and the polarization and ohmic losses were reduced by atomic layer deposition (ALD) at low temperatures. The hexagonal-pyramid array nano-structure was observed for the resulting micro-SOFC electrolyte membrane and a power density of 1.34 W/cm^2 at 500 °C was obtained [22]. Ramesh *et al.* demonstrated that co-doped ceria electrolytes offer high ionic conductivity for SOFCs at the intermediate temperatures [34].

Anode Materials

The anode is required to provide reaction sites for the electrochemical oxidation of the fuel gas. An appropriate anode has:

- A TEC same as that of the adjoining components and chemical compatibility with them;
- Fine particle size and the capacity to avoid coke deposition;
- Large triple phase boundary and high porosity (20–40%);
- High electrochemical activity for the oxidation of the selected fuel gas;
- Good electronic and ionic conductivity [12, 15].

Singhal *et al.* investigated that Ni-YSZ remains the best choice as anode material despite its high catalytic activity that limits its use for higher hydrocarbons where alternative materials like ceria or strontium titanate and copper cermet anodes for IT-SOFC may be used. Also ceramic anodes like doped perovskites along with ceria have been suggested despite some drawbacks [11]. Steele *et al.* reported that the use of nickel metal may lead to a deleterious volume reaction due to the formation of NiO. So redox stable and electronic conducting oxides may replace Ni or alternative anodes for anodic oxidation of hydrocarbons directly may be used at intermediate temperatures [14]. Badwal *et al.* in 2001 reported that the stability and performance of anode at the operating temperatures is greatly influenced by microstructure of the cermet. Alternative materials need to be explored to avoid the deteriorating anode performance due to possible Ni particles agglomeration and Ni dewetting of zirconia [6]. Haile *et al.* investigated that it is compulsory to limit the concentration of Ni to avoid coking and ceria must be incorporated into the anode cermet for better anode performance [33].

Taroco *et al.* demonstrated that Ni to YSZ volume ratio affects the conductivity of the material. The Ni/YSZ composite is not a good option for ethanol, methanol like fuel based SOFCs, because of its low acceptance to sulfur and particulate matter deposition. To avoid this the operating temperature can be reduced or by the choice of alternative anode materials like Cu-anodes alloyed with another metal like nickel or new perovskite materials like LSCFO-GDC and LSCM or LST (for IT-SOFC) [3]. Ringuede *et al.* showed that SOFCs which utilize Ni-YSZ cermet anodes are prone to sulphur poisoning as low as 2 ppm H_2S at 1273 K. In their work it was found that the performance loss can be reversed at H_2S concentrations to less than 15 ppm [23]. Ralph *et al.* reported that Ni-YSZ cermet is the most commonly used anode material that need proper equipment to remove sulphur from the fuels to avoid the poisoning of Ni sites. Due to percolation threshold of YSZ, CGO and CSO are being investigated as cermets with Ni microstructure [26]. McEvoy *et al.* explained the ongoing efforts to replace Ni with Cu or Co. The studies are on to investigate oxide based anodes such as reduced ceria or electronically conducting perovskites [28].

Interconnect

Interconnect is used to connect two fuel cells together so as to produce sufficient current and voltage. An interconnect must have the following characteristics:

- 100% electrical conductivity.
- No reaction with other cell components.
- Zero porosity.
- Thermal expansion compatibility.

Lanthanum chromite is the most commonly used material for interconnect of ceramic based SOFCs because it can withstand even unfavorable working conditions though it suffers from the problem of fabrication according to Ovenstone *et al.* [36]. Matasuzaki *et al.* reported that at elevated temperatures of about 900–1000 °C, interconnects like Inconel600 (a nickel based alloy) may be used [25]. McEvoy *et al.* suggested the optimum design target temperature of ferritic steel interconnector at about 700 °C [28]. Ralph *et al.* declared that ferritic steels may be efficiently used at or below 800 °C as they are cheaply and easily available. Also, the oxide scale problem can be overcome by either alloying the ferritic steel alloys by Ni or Co ions, or by coating the surface with a conductive ceramic [26]. Singhal *et al.* mentioned that at the high temperatures above 800 °C, doped lanthanum chromite ceramic is found to satisfy above requirements of the interconnect, but at temperatures less than 800 °C metallic alloys may be used efficiently in terms of low cost and easy manufacture, e.g., ferritic stainless steels like crofer22 and ZMG232. To solve the problems of Cr evaporation, electrical resistance and corrosion when exposed, surface coatings can be applied over the metallic alloy interconnects [11]. Badwal *et al.* suggested thick impermeable conductive and protective coatings having good chemical compatibility, and low Cr and oxygen ion diffusion coefficients on the metallic interconnect materials [6]. Tietz *et al.* studied the effect of applying the protective layers of LaCrO₃ in lowering the chromium vapor deposition on the cathode. Gettering may also help in neutralizing the Cr atoms in the coated layers. Cr₂Fe₂O₃. Chromium based interconnect has shown this recent development [9].

Effect of Processing on the Properties of Component Materials

Ovenstone *et al.* prepared three perovskite ceramics Ca doped lanthanum chromite, strontium doped lanthanum chromite and strontium doped lanthanum manganite by emulsion processing. EDX has proved that unsinterable powder may be formed due to small stoichiometric changes [36]. Tietz *et al.* reported that cost, automation, precision of various techniques and reproducibility are the factors that determine the fabrication processes. Various methods like tape casting, screen printing, warm processing, wet powder spraying and tape calendaring, laser ablation, colloidal deposition, CVD, electrophoresis or multiple spin coating may be used [9]. Suci *et al.* tried a new modified sol-gel method for preparing 7SvSZ and 11ScSZ nanoparticles to be used as electrolytes by using sucrose and pectin. Their conductivities were found to vary at temperatures lower than 400 °C [35]. Bujalski *et al.* discussed a number of techniques for making thin (5–20 μm) YSZ electrolytes, viz., sputtering, dip coating, spin coating, spray pyrolysis, electrophoretic deposition, slip casting, plasma spraying, electrostatic assisted vapor deposition, vacuum evaporation, laser spraying, transfer printing, sedimentation method, and plasma metal organic chemical vapor deposition [31]. Boldrini *et al.* prepared La_{0.80}St_{0.20}Ga_{0.83}Mg_{0.17}O_{2.815} by two methods – a conventional and a microwave assisted sol-gel Pechini method. MWA-SGP method showed ionic conductivity values higher than those checked for SGP samples. This clearly explains the vital role of microwave processing on lesser time and costs, but it also improves the electrolyte properties [24]. Chao *et al.* reported that MEMS allows the fabrication of very thin electrolytes. Various techniques like physical vapor deposition and atomic layer deposition were used to reduce the YSZ electrolyte thickness to tens of nanometers [22].

Various processing techniques for different fuel cell types are suggested in Table 3:

Table 3: Fabrication Methods for Various Types of Fuel Cell Concepts and Their Components [45].

Design	Fabrication method electrolyte	Electrode	Interconnect
Tubular Concept	CVD/EVD, plasmaspraying	Slurry coating, plasma spraying, CVD/EVD	EVD, plasma spraying
Monolithic	Calendar rolling, laminating, co-sintering	Calendar rolling, laminating, co-sintering	Calendar rolling, laminating, co-sintering
Planar	Tape casting, calendar rolling	Screen printing, slurry coating	Ceramic or metal processing

II. CONCLUSIONS

The work of SOFCs acknowledges and emphasizes man's endeavor to adapt to reduce the cost, to generate power densities as high as possible and for the long term durability and reliability. For these newer areas of exploration, a number of materials have been explored and tested that can replace the conventional

materials without deteriorating the fuel cell performance. Apart from the composition, optimization of synthesis process is further needed in the microstructure in order to fabricate the SOFCs cost effectively.

REFERENCES

- [1] Ramesh S, Reddy V. *Electrical Properties of Co-doped Ceria Electrolytes* 2009.
- [2] Singhal S. C. Solid Oxide Fuel Cells for Stationary, Mobile, and Military Applications. *Solid State Ionics* 2002; 152: 405–410p.
- [3] Taroco H. A, Santos J. A. F, Domingues R. Z., et al. Ceramic Materials for Solid Oxide Fuel Cells. *Advances in Ceramics – Synthesis and Characterization, Processing and Specific Applications* 2009; 423–446p.
- [4] Fergus J, Hui Rob, Li X, et al. (Eds). *Solid Oxide Fuel Cells: Materials Properties and Performance*. CRC Press. 2009.
- [5] Hirschenhofer J. H, Stauffer D. B, Engleman R. R., et al. *Fuel cell*, fourth Edn. 1998.
- [6] Badwal S.P.S. Stability of Solid Oxide Fuel Cell Components. *Solid State Ionics* 2001; 143: 39–46p.
- [7] de Souza S, Visco S. J, de Jonghe L. C. *J. Electrochem. Soc* 1997; 144: L35p.
- [8] Kim J.-W, Virkar A. V, Fung K.-Z, et al. *J. Electrochem. Soc* 1999; 146: 69p.
- [9] Tietz F, Haanappel V. A. C, Maim A, et al. Performance of LSCF Cathodes in Cell Tests. *Journal of Power Sources* 2006; 156: 20–22p.
- [10] Lamp P, Tachtler J, Finkenwirth O, et al., Development of an Auxiliary Power Unit with Solid Oxide Fuel Cells for Automotive Applications. *Fuel Cells* 2003; 3: 146–152p.
- [11] Singhal S.C. Solid Oxide Fuel Cells. *The Electrochemical Society-Interface* 2007; 41–44p.
- [12] Singhal S.C, Kendall K. *High Temperature Solid Oxide Fuel Cells: Fundamentals, Design, and Applications*. Elsevier Science Ltd., Oxford, UK; 2003.
- [13] Robert J. Braun, Sanford A. Klein, Douglas T. Reind. *Assessment of Solid Oxide Fuel Cells in Building Applications* 2001.
- [14] Steele B. C. H., Heintzel A. Materials for Fuel-Cell Technologies. *Nature* 2001; 414: 345–352p.
- [15] Florio D. Z. de, Fonseca F. C, Muccillo E. N. S, et al. Ceramic Materials for Fuel Cells. *Cerâmica* 2004; 50: 275–290p.
- [16] Shao Z, Haile S. M, Ahn J, et al. A Thermally Self-sustained Micro Solid-Oxide Fuel-Cell Stack with High Power Density. *Nature* 2005; 435: 795–798p.
- [17] Nesaraj S. A. Recent Developments in Solid Oxide Fuel Cell Technology – A Review. *Journal of Scientific and Industrial Research* 2010; 69: 169–176p.
- [18] Raza R, Wang X, Ma Y, et al. Improved Ceria–Carbonate Composite Electrolytes. *International Journal of Hydrogen Energy* 2010; 35: 2684–2688p.
- [19] Faro M. L., Rosa D. L., Antonucci V, et al. Intermediate Temperature Solid Oxide Fuel Cell Electrolytes. *Journal of the Indian Institute of Science* 2009; 89: 363–381p.
- [20] Dutta A, Mukhopadhyay J, Basu R.N. Combustion Synthesis and Characterization of LSCF-based Materials as Cathode of Intermediate Temperature Solid Oxide Fuel cells. *Journal of the European Ceramic Society* 2009; 29: 2003–2011p.
- [21] Kharton V. V, Marques F. M. B, Atkinson A. Transport Properties of Solid Oxide Electrolyte Ceramics: A Brief Review. *Solid State Ionics* 2004; 174: 135–149p.
- [22] Chao C.C, Hsu C, Cui Y, et al. Improved Solid Oxide Fuel Cell Performance with Nanostructured Electrolytes. *American Chemical Society* 2011; Article in Press.
- [23] Ringuede A, Labrincha J.A, Frade Jr. A. Combustion Synthesis Method to Obtain Alternative Cermet Materials for SOFC Anodes. *Solid State Ionics* 2001; 141–142p, 549–557p.
- [24] Boldrini S, Mortalò C, Fasolin S, et al. Influence of Microwave Assisted Pechini Method on La_{0.80}St_{0.20}Ga_{0.83}Mg_{0.17}O_{2.815} Conductivity. *Fuel cells* 2012; 54–60p.
- [25] Matasuzaki Y, Yasuda I. *Journal of the Electrochemical Society* 2001; 148A: 126p.
- [26] Ralph J.M, Kilner J. A, Steele B.C.H. New Materials for Batteries and Fuel Cells. *Proc. Symp.* San Francisco; 1999: 309p.
- [27] Ahn J. S, Omar S, Yoon H, et al. Performance of Anode-supported Solid Oxide Fuel Cell Using Novel Ceria Electrolyte. *J. Power Sources* 2010; 195: 2131–2135p.
- [28] McEvoy A.J. *Solid State Ionics* 2000; 132: 159–165p.
- [29] Sun C, Hui R, Roller J. Cathode Materials for Solid Oxide Fuel Cells: A Review. *J Solid State Electrochem* 2010; 14: 1125–1144p.
- [30] Winciewicz K.C, Cooper J. S. Taxonomies of SOFC Material and Manufacturing Alternatives. *Journal of Power Sources* 2005; 140: 280–296p.
- [31] Bujalski W. *Solid State Oxide Fuel Cells*. University of Birmingham; 2004.
- [32] Takahashi T., Esaka T, Iwahara H. *J. Appl. Electrochem* 1977; 7: 299p.
- [33] Haile S.M. *Acta Materials* 2003; 51: 5981–6000p.
- [34] Ramesh S, Vishnuvardhan C, Reddy. *Electrical Properties of Co-doped Ceria Electrolyte* 2009; 909–912p.
- [35] Suci C, Erichsen E.S, Hoffmann A.C, et al. Modified Sol-Gel Method Used for Obtaining SOFC. *Electrolyte Materials* 2009; 25(2): 1679–1686p.
- [36] Ovenstone J, Ponton C. B. Emulsion Processing of SOFC Materials. *Journal of Materials Science* 2000; 35: 4115–4119p.
- [37] Nerst W. US patent 685 730 (1902); filed 24/8/1899.
- [38] Baur E, Preis H. Z. *Elektrochem* 1937: 727p.
- [39] Button D. D, Archer D. H. *American Ceramics Society Meeting*, Washington, DC; 1996.
- [40] Rohr F. J. (Ed.). *Report BMFT-FBT 77-17*. German Research and Technology Ministry; 1977.
- [41] Spacil H. S. US Patent 3,503,809 (1970) filed 1964.
- [42] Brown J. T. *Energy* 1986; 11: 209p.
- [43] Faro M. L, Rosa D. L, Antonucci V, et al. *Journal of the Indian Institute of Science* 2009; 89.
- [44] *Fuel Cell Handbook*, Seventh Edition. EG&G Technical Services, Morgantown West Virginia, November 2004.
- [45] Badwal S. P. S, Foger K. *International Ceramic Monographs* 2002; 1(2): 761–765p.

Co-ordinator
IQAC, Shri Ram College,
Muzaffarnagar

Chairman
IQAC, Shri Ram College,
Muzaffarnagar



Try out **PMC Labs** and tell us what you think. **Learn More.**



JOURNAL OF CANCER

Home | Editorial board | Author info | Submit a manuscript

J Cancer, 2021; 12(16): 4891–4900.

Published online 2021 Jun 11. doi: [10.7150/jca.58582](https://doi.org/10.7150/jca.58582)

PMCID: PMC8247366

PMID: [34234859](https://pubmed.ncbi.nlm.nih.gov/34234859/)

Chlamydia Trachomatis Infection: Their potential implication in the Etiology of Cervical Cancer

Xingju Yang,¹ Anam Siddique,² Abdul Arif Khan,³ Qian Wang,⁴ Abdul Malik,⁵ Arif Tasleem Jan,⁶ Hassan Ahmed Rudayni,⁷ Anis Ahmad Chaudhary,⁷ and Shahanavaj Khan^{2,5,8,✉}

¹Department of Nursing, Jinan People's Hospital Affiliated to Shandong First Medical University, Jinan, Shandong 271199, China.

²Department of Biosciences, Shri Ram Group of College (SRGC), Muzaffarnagar 251001, India.

³Division of Microbiology, Indian Council of Medical Research-National AIDS Research Institute, Pune, Maharashtra, India.

⁴Department of Obstetrics and Gynecology, Jinan Fifth People's Hospital, Jinan, Shandong, 250022, China.

⁵Department of Pharmaceutics, College of Pharmacy, P.O. Box 2457, King Saud University, Riyadh 11451, Saudi Arabia.

⁶School of Biosciences and Biotechnology, Baba Ghulam Shah Badshah University, Rajouri 185236, India.

⁷Department of Biology, College of Science, Imam Mohammad Ibn Saud Islamic University (IMSIU), Riyadh 11623, Saudi Arabia.

⁸Department of Health Sciences, Novel Global Community Educational Foundation, Australia.

✉ Corresponding author: Dr. Shahanavaj Khan, E-mail: sdkhan@ksu.edu.sa; Tel.: +91-921-999-3262.

Department of Pharmaceutics, College of Pharmacy, P.O. Box 2457, King Saud University, Riyadh 11451, Saudi Arabia; Department of Biosciences, Shri Ram Group of College (SRGC), Muzaffarnagar 251001, India; Novel Global Community Educational Foundation, Australia.

Competing Interests: The authors have declared that no competing interest exists.

Received 2021 Jan 23; Accepted 2021 May 13.

Copyright © The author(s)

This is an open access article distributed under the terms of the Creative Commons Attribution License (<https://creativecommons.org/licenses/by/4.0/>). See <http://ivyspring.com/terms> for full terms and conditions.

Abstract

Pathogenic bacterial strains can alter the normal function of cells and induce different levels of inflammatory responses that are connected to the development of different diseases, such as tuberculosis, diarrhea, cancer etc. *Chlamydia trachomatis* (*C. trachomatis*) is an intracellular obligate gram-negative bacterium which has been connected with the cervical cancer etiology. Nevertheless, establishment of causality and the underlying mechanisms of carcinogenesis of cervical cancer associated with *C. trachomatis* remain unclear. Studies reveal the existence of *C. trachomatis* in cervical cancer patients. The DNA repair pathways including mismatch repair, nucleotide excision, and base excision are vital in the abatement of accumulated mutations that can direct to the process of carcinogenesis. *C. trachomatis* recruits DDR proteins away from sites of DNA damage and, in this



A brief molecular insight of COVID-19: epidemiology, clinical manifestation, molecular mechanism, cellular tropism and immuno-pathogenesis

Sweta Singh¹ · Rakesh Pandey¹ · Sarika Tomar¹ · Raunak Varshney² · Darshika Sharma^{1,3} · Gurudutta Gangenahalli¹

Received: 3 November 2020 / Accepted: 23 June 2021

© The Author(s), under exclusive licence to Springer Science+Business Media, LLC, part of Springer Nature 2021

Abstract

In December 2019, the emergence and expansion of novel and infectious respiratory virus SARS-CoV-2 originated from Wuhan, China caused an unprecedented threat to the public health and became a global pandemic. SARS-CoV-2 is an enveloped, positive sense and single stranded RNA virus belonging to genera betacoronavirus, of Coronaviridae family. The viral genome sequencing studies revealed 75–80% similarity with SARS-CoV. SARS-CoV-2 mainly affects the lower respiratory system and may progress to pneumonia and Acute Respiratory Distress Syndrome (ARDS). Apart from life-threatening situations and burden on the global healthcare system, the COVID-19 pandemic has imposed several challenges on the worldwide economics and livelihood. The novel pathogen is highly virulent, rapidly mutating and has a tendency to cross the species boundaries such as from bats to humans through the evolution and natural selection from intermediate host. In this review we tried to summarize the overall picture of SARS-CoV-2 including origin/ emergence, epidemiology, pathogenesis, genome organization, comparative analysis with other CoVs, infection and replication mechanism along with cellular tropism and immunopathogenesis which will provide a brief panoramic view about the virus and disease.

Keywords SARS-CoV-2 · COVID-19 · Pandemic · Infection · Pathogenesis

Introduction

Recent mysterious pneumonia that spread worldwide and known to have an origin at the seafood and animal market, in Wuhan, China has become global pandemic and given the name “2019-nCoV” by World Health Organization (WHO). Further, the International Committee of Virus Taxonomy

classified this new virus as SARS-CoV-2 (Severe Acute Respiratory Syndrome coronavirus) based on standard practice, pathology, phylogeny and taxonomy [1]. SARS-CoV-2 known to be originated from bat coronavirus and transmitted to humans due to its ability to cross species barrier from bats to humans [2]. In the past two decades, coronaviruses are responsible for the three epidemics namely COVID-19, SARS and MERS. This novel SARS-CoV-2 is a zoonotic virus, belong to Coronaviridae family of Nidovirales order [3]. This family got its name “coronavirus” because of the crown-like appearance of its spike protein. The Coronavirus family is composed of four subgroups i.e. alpha (α), beta (β), gamma (γ) and delta (δ). Two subgroups the alpha (α), beta (β), mainly affect mammals, whereas the other two subgroups, gamma (γ) and delta (δ) primarily affect birds [4]. Till date, seven kinds of human coronavirus have been identified out of which two belongs to alpha (α), HCoV-NL63 and HCoV-229E and five belongs to beta (β) HCoV-OC43, HCoV-HKU1, SARS-CoV (severe acute respiratory syndrome corona virus), MERS-CoV (Middle East respiratory syndrome coronavirus) and SARS-CoV2. The size of

Rakesh Pandey and Sarika Tomar have contributed equally to the work.

✉ Gurudutta Gangenahalli
gurudutta.inmas@gmail.com

¹ Division of Stem Cell and Gene Therapy, Institute of Nuclear Medicine and Allied Sciences, Brig. S. K. Mazumdar Road, Delhi 110054, India

² Division of Cyclotron and Radiopharmaceutical Sciences, Institute of Nuclear Medicine and Allied Sciences, Brig. S. K. Mazumdar Road, Delhi 110054, India

³ Meerut Institute of Engineering and Technology, Meerut, India

Published online: 30 June 2021

Co-ordinator
IQAC, Shri Ram College,
Muzaffarnagar

Chairman
IQAC, Shri Ram College,
Muzaffarnagar

Springer

corona viruses range from 65 to 125 nm in diameter with a crown-like feature on the exterior surface. Genetically, Coronavirus is single-stranded positive-sense RNA with a relatively larger genome composition of 26 to 32kbs. Its genome composed of 6–10 open reading frames (ORFs), in which first ORF constitutes largest part of genome and other ORFs encode accessory and structural proteins. SARS-CoV-2 is different from SARS-CoV as seen in phylogenetic report and genomic sequencing. During last one year, it has become more virulent by undergoing frequent mutation thereby making it difficult to associate a particular strain with the severity of the disease. The binding of virus to host cell is the main determinant for the viral pathogenesis and designing of any antiviral therapy. Angiotensin-converting enzyme (ACE2) a Type I membrane glycoprotein which is highly up-regulated in the lungs and endothelial cells acts as a primary receptor for the viral entry and physiologically important in the progression of COVID-19 disease and illness [5]. This virus mainly affects the lower respiratory system and causes pneumonia similar to other beta coronaviruses SARS-CoV and MERS-CoV. Apart from the lower respiratory system it is also affecting gastrointestinal system, liver, heart, and kidney and leading to multiple organ failure [6, 7]. The extra pulmonary manifestations such as diarrhoea, impaired liver

function, chronic renal disease etc. suggests viral tropism/affinity for the non-pulmonary tissues [5].

Epidemiology

The novel coronavirus, SARS-CoV-2 outbreak that started from Wuhan, China in December has been globally spread and imposed a severe threat to the people's health. China, the epicenter of the COVID-19 pandemic reported 4653 deaths and 89,000 confirmed cases. As per WHO latest report, more than 200 countries are threatened with more than 146 Million confirmed cases and over 3.1 Million deaths globally (Fig. 1) while more than one billion patients have given vaccine doses (232 Million fully vaccinated). Apart from life-threatening situations and huge burden on the global healthcare system, the COVID-19 pandemic has imposed several other challenges on economy, livelihood, individual freedom and social life. Besides confirmed cases; millions people were in quarantine/isolation for several months. To combat the pandemic, several countries have posed nationwide/statewide lockdown. Still several countries and states are in lockdown or under some sort of curb/curfew as world is witnessing second/third wave. Worldwide lockdown has

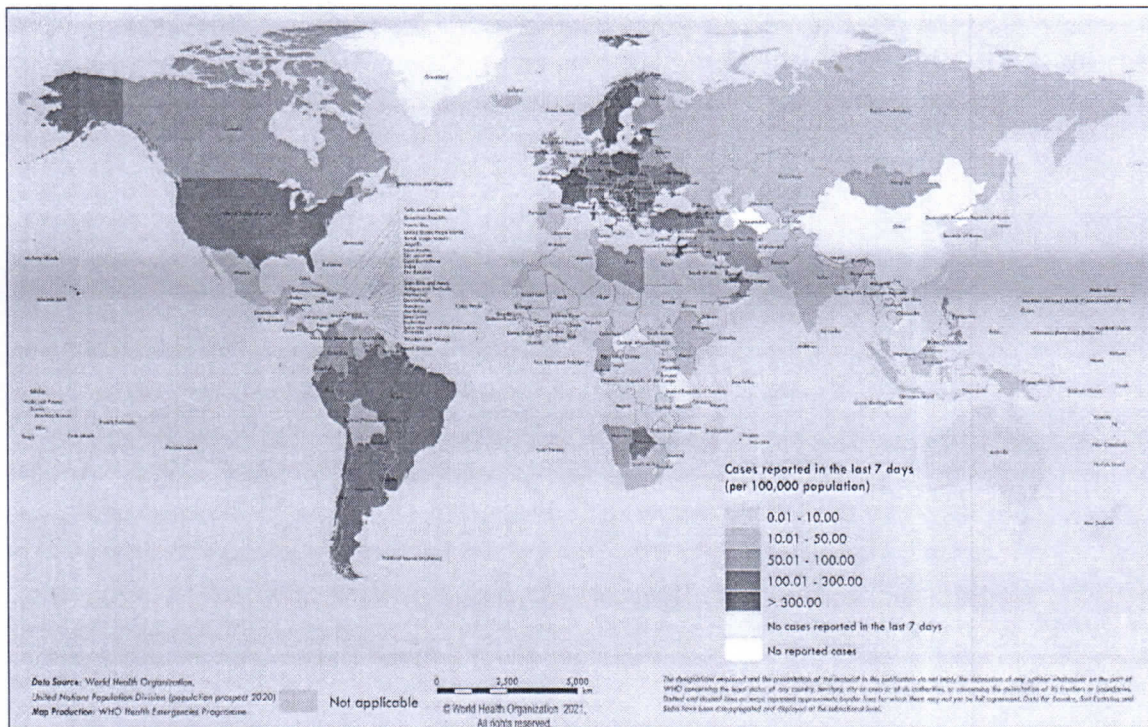


Fig. 1 Countries, territories or areas with reported confirmed cases of COVID-19, 30 March 2021 (Source: www.who.int/emergencies/diseases/novel-coronavirus-2019/situation-reports)

imposed different kinds of psychological challenges among people and also affected the livelihood of millions.





Symptoms, age, sex and CFR

The recent outbreak of pandemic COVID-19 is known as a respiratory disease caused by SARS-CoV-2 (<https://www.who.int/westernpacific/emergencies/COVID-19>). Chinese Centre for Disease Control and Prevention (China CDC) published a detailed analysis of 44,672 confirmed cases on February 14th. The clinical manifestations of COVID-19 could be both asymptomatic and symptomatic that include fever, sore throat, dry cough, tiredness, shortness of breath, ARDS (Acute respiratory distress syndrome), and pneumonia with varying degrees of severity. Complaints of gastrointestinal symptoms such as diarrhoea, nausea and vomiting, and myalgia or fatigue are also seen during illness [8–14]. The estimated CFR (case fatality rate) for COVID-19 is 3.4% up to March which is much higher than the flu (Fig. 2). As per the China CDC, 14% of patients were severe while 81% of patients showed only mild symptoms i.e. non-pneumonia and mild pneumonia, and no death was reported in this case [15]. 49.0% CFR was reported in 5% critically ill with respiratory failure, septic shock, and multiple organ failure. Total CFR was 2.3% while out of total fatality only 2.2% of patients were below 20 years. As per various reports children appeared to be at lower risk. CFR in the age group 70–79 was 8%

while it was 14% in the age group 80 and above. Higher CFR was reported among the patient with pre-existing chronic ailments such as cardiovascular disease (10.5%), diabetes (7.3%), chronic respiratory disease (6.3%) and hypertension (6%). Variable CFR has been seen based of region/country. Variable CFR has been seen based of region/country. Variability in CFR would be very common as its depends on many factors such as socioeconomic condition, healthcare infrastructure, level of preparedness, population, co morbidity in population, testing capacity per million etc. in the particular country.


Till the date, no sex-disaggregated data on SARS-CoV-2 susceptibility towards infection and both males and females are equally infected with COVID-19. However, there is few reports on sex disaggregated data on mortality and vulnerability towards the disease that suggest that male mortality is higher than female. As per one report published in Lancet, male to female ratio was found to be 80% to 20% (median age of 79.9 years for men and women for 83.4 years for women) [16]. Another report stated that male patient were more severely affected than female ($P=0.035$) and mortality of male were 2.4 times higher than female (70.3 vs. 29.7%, $P=0.016$) [17].

Low rate mortality in women could be due to sex-based immunity, low smoking, and drinking as compared to men. However, there is no conclusive understanding yet as sex-disaggregated data are insufficient and it would be too early to conclude anything at this stage.

Disease	Flu	COVID-19	SARS	MERS
Disease Causing Pathogen	 Influenza virus	 SARS-CoV-2	 SARS-CoV	 MERS-CoV
R_0 Basic Reproductive Number	1.3	2.0 - 2.5 *	3	0.3 - 0.8
CFR Case Fatality Rate	0.05 - 0.1%	~3.4% *	9.6 - 11%	34.4%
Incubation Time	1 - 4 days	4 - 14 days *	2 - 7 days	6 days
Hospitalization Rate	2%	~19% *	Most cases	Most cases
Community Attack Rate	10 - 20%	30 - 40% *	10 - 60%	4 - 13%
Annual Infected (global)	~ 1 billion	N/A (ongoing)	8098 (in 2003)	420

* COVID-19 data as of March 2020.

Fig. 2 Epidemiological comparison of respiratory viral infections


Co-ordinator
IQAC, Shri Ram College,
Muzaffarnagar


Chairman
IQAC, Shri Ram College,
Muzaffarnagar

Incubation period

The incubation period is crucial information for active healthcare monitoring and taking proactive measures to stop the spreading. One of the very first reports estimated a mean incubation period of 5.2 days based on ten confirmed cases [18]. Another report claimed the median incubation period of 4.75 (interquartile range: 3–7.2) days based on the study of 125 patients with confirmed exposure [19]. A study based on 158 confirmed cases reported a median incubation period of 5.0 days (CI, 4.4 to 5.6 days) [20]. However, estimation on incubation period based large sample size suggested only 3.0 days median incubation period and could be as long as 24 days [21]. There is strong possibility that this RNA virus invades the host innate immune system, a first-line host defence, to evade immune detection. Also, genetic variation plays an important role in the variable host immune response. These may be the reasons behind the long and variable incubation period. There is a possibility that a high incubation period plays a role in the degree of pathogenicity.

A study performed on 1099 patients to determine the viral load and transmission potential during the incubation period in both symptomatic and asymptomatic patients found to be higher soon after the onset of symptoms similar to influenza [22]. Viral load in both symptomatic and asymptomatic patients was quite similar indicating the transmission potential of both asymptomatic patients as well as symptomatic patients 2–3 days prior to the onset of symptoms. The role of asymptomatic patients in the transmission of infection is yet to be defined. Larger cohorts data will be needed to understand the disease and transmission dynamics. However, primary reports/studies led countries to strategies different measures such as quarantine, isolation and tracing/testing to minimize the transmission.

Origin and reservoir

Recent genomic data indicate that the most closely related virus to SARS-CoV-2 originated from bats [23–25]. Genomic sequence of sampled virus from bat from Yunnan province approximately 1500 km away from epicentre Wuhan showed 96%–97% similarity with SARS-CoV-2. Practically these viruses will take almost 15–20 year to evolve to SARS-CoV-2 which suggests the possibility of multiple intermediate hosts. Current findings suggest that bats are most anticipated reservoir hosts for SARS-CoV-2, but there is a strong possibility of ‘intermediate’ host that augmented SARS-CoV-2 to acquire some desired

mutations to become virulent to human transmission as it happened in case of MERS and SARS where camels and civets were intermediate hosts, respectively. MERS-CoV was supposed to be present in camels for almost a decade and through multiple cross-species transmission, it appeared in humans. A strong possibility is that these animals could be true reservoir hosts of SARS-CoV-2 [26].

Another intriguing finding is that none of bat corona virus sequenced from Hubei province was found close to SARS-CoV-2 in phylogenetic trees. [27] One interesting report revealed that the virus found in Malayan pangolins (*Manis javanica*) is closely related to SARS-CoV-2 and showed strong similarity to the RBD sequence of SARS-CoV-2 along with six key residues important for ACE2 receptor binding. However, the rest of the genome of SARS-CoV-2 was distant from this pangolin-associated coronavirus. This study suggests that pangolins could be another possible intermediate host in the rise of novel SARS-CoV-2 outbreak. Closest bat CoV RaTG13 virus genomic sequence showed 96–97% similarity with SARS-CoV-2 though spike protein diverges in bat virus. Natural selection is currently the most probable answer for the origin of SARS-CoV-2 infecting a primary and intermediate hosts and finally reaching to humans. However, current findings and research are not sufficient to provide complete information on natural host or intermediate host of SARS-CoV-2.

Peculiar features, mutation and insertion in SARS-COV-2 genome

Genome Organization and predisposition

SARS CoV-2 as other corona viruses belong to the order Nidovirales and family Coronaviridae of the betacoronavirus genera [28]. SARS-CoV-2 is a single stranded positive sense virus having 29,891 nucleotides (G+C = 38%) encoding 9860 amino acids. Its genome contains two untranslated region (UTR) and one long open reading frame (ORF) that codes for the polyprotein. S protein of SARS-CoV-2 is also distinct from other coronavirus in the subgenus Sarbeco virus [29]. S protein of SARS-CoV-2 possess a size of 1273 amino acids while it is 1255 amino acids and 1245–1269 amino acids in case of SARS-CoV and bat SARS-CoV. In term of sequence similarity, SARS-CoV-2 S protein has 76–77% similarity from civet and human but surprisingly higher similarity 90.7–92.6% with pangolin coronavirus [30].

The sequential arrangement of genes from 5′-3′ is ORF1a, ORF1b, S, ORF3, E, M, and N in SARS-CoV-2 which is distinct in its genera [31] (Fig. 3). Also, SARS-COV-2 lacks the hemagglutinin esterase gene which is present as a component of the structural gene in SARS-CoV

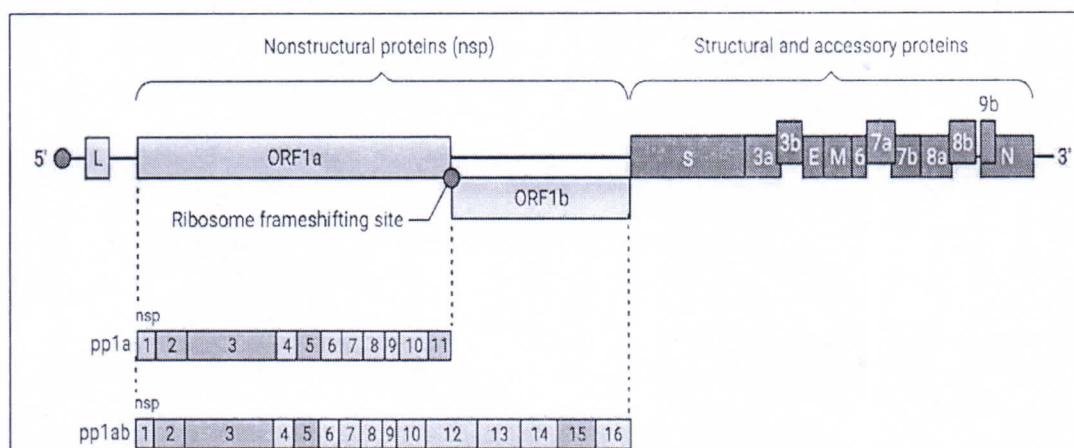


Fig. 3 Genome organization of SARS-CoV-2

Table 1 Comparison of proteins of SARS-CoV and SARS-CoV-2

Proteins	SARS-CoV	SARS-CoV-2
8a	Present	Absent
8b	Shorter, 84aa	Longer, 121aa
3b	Longer, 154aa	Shorter, 22aa

and MERS-CoV [29]. There are no major differences in the nsps and ORFs of SARS-CoV-2 and SARS-CoV except at some particular proteins [32]. Recent works reported 116 mutations along with three common mutations in the ORF1ab gene at C8782T, in the ORF8 gene at T28144 C and in the N gene at C29095T based on bioinformatics analysis of 95 complete genomic sequence of SARS-CoV-2 available till 05 April 2020 [33]. Pp1ab is the first ORF starting from 5' end which encodes a nonstructural protein of size 29844 bp, 29751 bp, and 30119 bp in SARS-CoV-2, SARS-CoV and MERS-CoV respectively. The length of spike protein is significantly different in CoVs. The length of spike protein at the 3' in SARS-CoV-2 is 1273aa while 21493aa and 1270aa in SARS-CoV and MERS-CoV respectively [31].

A comparative analytical study of the transmembrane region of SARS-CoV-2 nsp2 and nsp3 with SARS-CoV revealed that mutation occurs at 723aa (glycine to serine) and 1010aa (isoleucine to proline) positions [34]. The functional significance of these changes is still unknown but these are mostly related to the virulence of the virus.

Nsp7, nsp13, E protein, and accessory proteins p6, 8b do not show any mutation. As evident by the genomic similarity of SARS-CoV-2 with SARS-CoV, the amino acid organization is also quite similar except some notable differences in the accessory proteins present at the 3' end [35] (Table 1).

High affinity to angiotensin converting enzyme 2 (ACE-2)

The crystal structure revealed that SARS-CoV RBD is composed of two major structures: a core structure and a receptor-binding motif (RBM) that binds to the outer surface of the ACE2 receptor [36]. Further, another study demonstrated that SARS-CoV-2 bound strongly to human and bat ACE-2 and even inhibited the binding of SARS-CoV to ACE-2 [37]. Sequence alignment studies of the amino acid (aa) of SARS-CoV-2 S protein with SARS-CoV S protein revealed [38, 39] the complete structural and functional domain in SARS-CoV-2 S protein. S1 segment (aa14–685) consists of N-terminal domain (aa14–305), RBD (aa319–541) along with RBM (aa437–508) and S2 segment (aa686–1273) consists of fusion domain (aa788–806), HR1 (aa912–984), HR2 (aa1163–1213), TM domain (aa1214–1237) and cytoplasmic domain (aa1238–1273) [40]. Residues from 318 to 510 in the S1 region are enough for high-affinity binding to the peptidase domain of ACE2 [41]. Sequence alignment study between SARS-CoV-2 and SARS-CoV spike has revealed that they share 76% to 78% identity in the whole spike protein and approximately 73% to 76% identity in the receptor binding domain and around 50% to 53% similarity in RBM. [36].

A total of 27 amino acid substitutions have been discovered in spike protein which comprises of 1273 amino acids. Six amino acid residues L455, F486, Q493, S494, N501 and Y505 in SARS-CoV-2 which corresponds to Y442, L472, N479, D480, T487 and Y491 in SARS-CoV RBD, are crucial for ACE2 receptor binding. Out of six crucial amino acid residues five are substituted in SARS-CoV-2 [37, 42–44]. Detailed analysis of S protein indicates longer capping loop (responsible for electrostatic interaction) and greater protein–protein contact result in the enhanced

[Signature]
Co-ordinator
IQAC, Shri Ram College,
Muzaffarnagar

[Signature]
Chairman
IQAC, Shri Ram College,
Muzaffarnagar

binding capability of SARS-CoV-2 (-15.7 kcal/mol) in comparison to SARS-CoV (-14.1 kcal/mol) [45]. These amino acid substitution and greater protein contact found in the hotspot area of the spike protein may indicate the effect of natural selection in increasing the affinity of the SARS-CoV-2 toward human ACE2[46].

Other six substitutions in the amino acid residue 569–655 of the SD segment present in S1 subunit have been discovered. Host range and affinity of RBD are critically determined by six RBD amino acids. Four notable substitutions have been seen in two peptides that were served as antigen in C-terminal in S1 subunit (Q560L, S570A, F572T, and S575A) [35, 47].

Very recent work based on the isolate from 11 random patients, observed total 33 mutations out of which 19 were new and not reported before including six mutations in the spike S protein. Further, it showed that these mutations lead more cytopathogenicity and viral load in the Vero-E6 cells. This finding suggests that the virus is capable of varying its pathogenicity and virulence in a short time frame [48].

Presence of polybasic furin cleavage site and N-glycan shielding

Another unique feature of the SARS-COV-2 genome is the insertion of a polybasic furin cleavage site at the S1/S2 interface of spike protein which is missing in all other SARS/ SARS-CoV [42, 49]. Furin is a proteolytic enzyme that is responsible for the cleavage of basic amino acids. Activation and priming by furin-like proteases are the signatures of several pathogenic viruses [50]. Addition of a polybasic cleavage site helps in the cell–cell fusion without altering the viral entry into the cell [50].

Amino acid alignment-based bioinformatics study of the S glycoprotein of SARS-CoV-2 revealed the insertion of furin cleavage sites in the sequence. Surprisingly, the most closely related bat CoV, RaTG-13 doesn't have the furin cleavage site [51] Since, furin proteases are abundant in the respiratory tract, it is hypothesized that SARS-CoV-2 S glycoprotein is separated upon exit from the epithelial cells and therefore can effectively target different cells and can increase the virulence.

Glycan shielding is a critical feature of SARS-CoV-2 having great importance in the context of vaccine designing. Virus uses glycan shielding strategy to evade the host immune system by masking the spike glycoprotein (S protein) through extensive glycosylation. Thick coating of carbohydrate on highly immunogenic epitope of the virus is a classic example of escaping from the host immune responses [52, 53]. Glycosylation pattern of SARS-CoV and SARS-CoV-2 is different from other RNA virus such as HIV in having greater concentration of N-glycan in comparison to O-glycans [54]. SARS-CoV-2 has 22 speculated

glycoprotein sites per promoter on the spike protein out of which 17 have been proved to be already preoccupied [54].

Mechanism of virus invasion in host cell

The viral proteins that mediates SARS-CoV-2 entry and fusion and replication into host cells share a similar structure with those of SARS-CoV. Sequencing of COVID-19 shows 79.5% sequence similarity to SARS-CoV, 51.8% with MERS-CoV, and shares 96% structural identity across the whole genome to a bat coronavirus [38, 55].

Virus attachment and fusion

SARS-CoV-2 has the conventional coronavirus structure with spike glycoprotein, nucleocapsid protein, envelope glycoprotein, membrane glycoprotein, lipid bilayer, and genomic RNA. The CoV spike (S), which is classified as type I viral fusion protein [56], synthesized as 1300 amino acids containing single-chain precursor followed by folding and trimerization [56], plays pivotal role in viral attachment, fusion, and entry to the host cell. The binding between RBD of the spike protein of the SARS-CoV-2 to host ACE2 receptor (angiotensin-converting enzyme 2), is important for viral entry into the host body similar to SARS-CoV [55].

There are two domains of viral S glycoprotein that recognize a variety of host receptors leading to viral attachment (S1) and fusion (S2) domain to host cell. The spike protein, an anchor machinery, present on the surface of coronavirus as homotrimers protruding from the viral surface mediates its entry into the host cell through receptor binding domain (RBD) in S1 subunit. [57] It is reported in many studies on CoVs that S is cleaved at the host surface between the S1 and S2 subunits before fusion, however they remain non-covalently bounded and this confirmation is considered as closed prefusion conformation. [58–62] Further, host proteases cleave S protein, at S2 site, very close and upstream to fusion peptide [63, 64] that lead to activation the protein for membrane fusion through irreversible fusion favourable conformational changes [60, 61, 65–67]. Virus entry into the host cell is complex and orchestrated between both viral and host cell (Fig. 4).

RBD in S1 of SARS-CoV-2 spike protein strongly binds to human ACE 2 and is a key player of virus host range and cellular tropism. Recent evidences by Cryo-Electron Microscopy have affirmed that SARS-CoV-2 S protein binding affinity to ACE2 is approximately 10–20 times greater than those of SARS-CoV S protein. [41, 68] The other subunit of S protein i.e., S2 is enriched with alpha helices and mediates viral-host cell membrane fusion by two tandem domains naming heptads repeats 1 (HR1) and 2 (HR2). The fusion domain contains a fusion peptide composed of 15–25

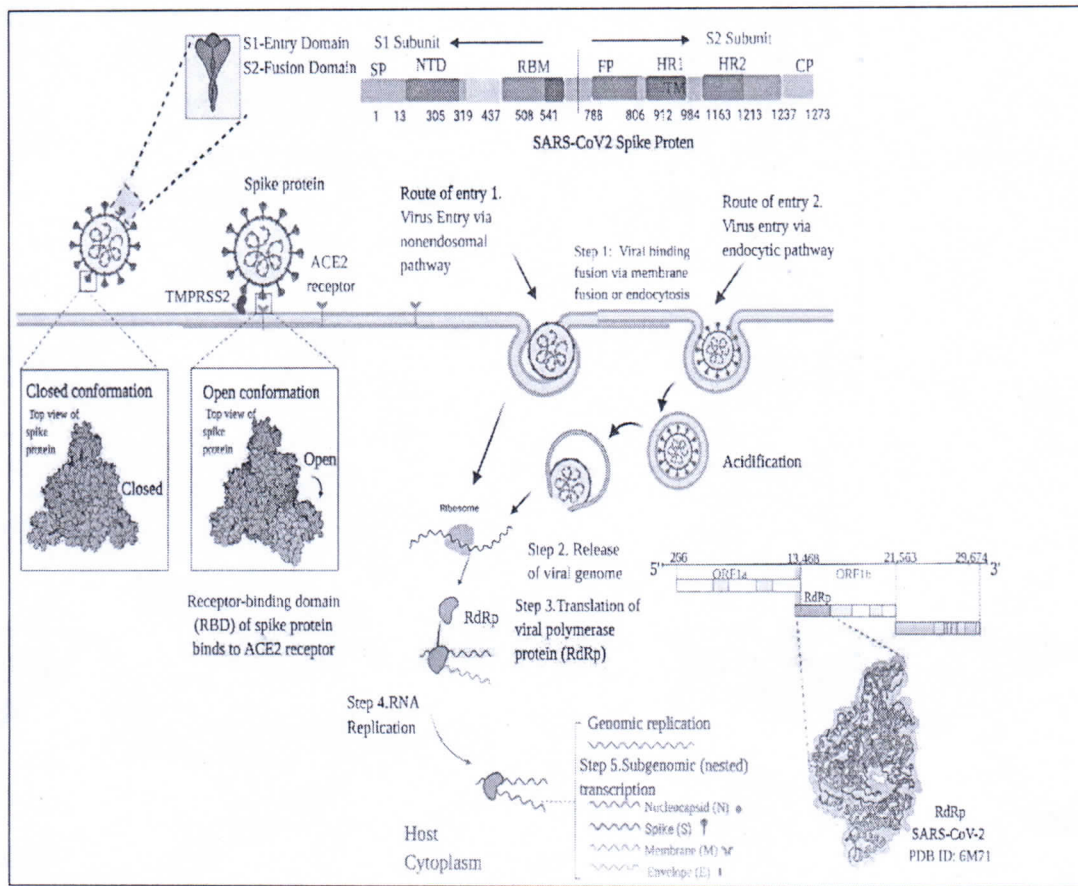


Fig. 4 SARS-CoV-2 Spike protein conformation, entry, fusion and replication. 1 SARS-CoV-2 interacts with host's ACE2 receptors and transmembrane protease serine 2 protein (TMPRSS2) through the spike protein. 2 It is followed by two entry pathways either A. non-endosomal or B. endocytic pathway or both to enter the host cell. 3.

Soon after its entry into host cell, it releases its genome and overtake protein synthesis machinery of host cell and start the translation of RdRp 4 Afterward SARS-CoV-2 replication and transcription are catalyzed by RdRp

hydrophobic amino acids. There are two distinct structural conformations of spike protein, before and post fusion which indicates the presence of some triggering mechanism for transition of confirmation.

The second step of viral infection is fusion with the host cellular membrane. Based on structure and function viral fusion proteins are classified into three types (I, II, and III). [69, 70] Based on structural features of fusion domain and requirement of protease cleavage to form fusogenic conformation and presence of HR1 and HR2 to form 6-HB, the coronavirus S protein is classified as class I fusion protein [56]. Fusion machinery, S2, is enriched with alpha helices and mediates viral-cell membrane fusion with the help of two tandem domains naming heptads repeats 1 (HR1) and 2 (HR2) and S2 subunits of SARS-CoV-2 and SARS-CoV shows 88% sequence identity. HR1 and HR2 domain of S2 subunit interact with each other that lead to the formation of 6-helix bundle (6-HB) fusion core, which brings viral and

host cellular membranes in close proximity for fusion and subsequently leads to the entry of virus in host cells. Four conformational changes happen throughout fusion process (1) Pre-fusion structural conformations (2) pre-fusion meta-stable conformation (3) pre hair-pin confirmation (4) post fusion stable state, which indicates the presence of some triggering mechanism for transition of confirmation. It is reported in many studies on CoVs that S protein is cleaved at host surface with protease between the S1 and S2 subunits before fusion however, they remain non-covalently bounded and this confirmation is considered as closed meta-stable prefusion conformation. [56, 59–64] Host proteases cleave S protein, at S2', very close and upstream to fusion peptide [64, 65] that lead the activation of the protein for membrane insertion through pre-hairpin intermediate state an irreversible fusion favourable conformation [59, 62, 63, 66, 67]. A recent study demonstrates that priming of SARS-CoV-2 S proteins by host cell serine protease TMPRSS2 and

[Signature]
Co-ordinator
IQAC, Shri Ram College,
Muzaffarnagar

[Signature]
Chairman
IQAC, Shri Ram College,
Muzaffarnagar

endosomal cysteine proteases CatB/L, vital for viral entry into host cells, mediate through S protein cleavage at S2' site at S1/S2 interface. [71] After insertion of the FP domain, the HR1 regions rearranged to form coiled trimer and facilitate the binding hydrophobic grooves with three HR2 regions antiparallely [72]. This rearrangement of HR1 and HR2 forms fusion core 6-HB, which leads to viral and host cell membranes into close proximity for fusion and forms the last stable post-fusion state. The last step of fusion process happens through two stages hemi-fusion stage and pore formation. [73] In a nutshell, virus entry into the host cell is complex and orchestrated between both viral and host cell. Presence and availability proteases involve in priming on target cells play a key role in determining whether CoVs penetrate inside cells through the plasma membrane or endocytosis pathway.

Replication

Replication machinery has a conserved organization at 5' end (including nonstructural protein) and 3' end (including structural protein). The viral replication is initiated when S protein binds to the ACE2 receptor inducing a conformational change which results in the endocytosis of the virus causing the release of viral ssRNA genome into the host cytoplasm [67].

The corona virus replication process could be divided into three parts: (1) translation of viral genome (ssRNA) to make necessary protein for genome synthesis (2) Simultaneous transcription and translation process (3) Assembly of viral genome and protein (Fig. 4). The SARS-CoV-2 replicase gene present on the 5' end make around 2/3 of the genome and consists of two 2 ORF, ORF1 and ORF2 which further code for two co-terminal polyproteins pp1a and pp1a respectively [29, 74]. For the expression of these two polyproteins, slippery sequence (5-UUUAAAC-3) and RNA pseudoknot is essential for ribosomal frameshifting from the repla reading frame into replb ORF. These polyproteins are subsequently cleaved in distinctive nonstructural protein (nsp). Cleavage of giant polyprotein mainly done by two proteases, papain-like (PLpro or nsp3) and chymotrypsin like (3CLpro or nsp5) into 16 nsp. ORF1a encode nsp1 to nsp11 and ORF1b encodes nsp12 to nsp16. The 3' part of the genome encode for 13 ORF's which include 4 structural proteins and 13 accessory proteins.

The second step is the organization of nsp 7, 8, and 9 at 3'end of genomic RNA to form membrane-associated replicase–transcriptase complex (RTC) where nps8 primase initiate RNA synthesis that finally leads to change in confirmation of 3'RNA (BSL to PK). This conformation change recognized by RdRp and helicase (nsp13) and other related factors like processing (nsp7 and nsp8), proofreading (nps10 and nps14)) and allow the synthesis of negative

stranded RNA to replication and translation of genomic and subgenomic RNA. Further, this negative strand RNA can take two pathways 1. Replication into genomic positive sense RNA or 2. Discontinuous transcription into several subgenomic mRNA that can be translated into different proteins [75].

In discontinuous transcription small subgenomic RNA are transcribed through premature termination during the synthesis of the negative-strand RNAs when preceding viral gene, TRS-B, jump and bind to the TRS-L of parent RNA. Long distant interaction TRS-B of preceding gene and 5' TRS-L of parent RNA is mediated through RNA–protein complex as complex bring them in close proximity. [76–78]. This whole process of replication happens in DMV (double membrane vesicle) and CM (convoluted membrane). SARS-CoV electron tomography analysis demonstrated that it forms a unique reticulovesicular network with which both viral replicase subunits and ssRNA were associated [79].

Recent studies reveal that DMVs are originated from ER and nps4 and nps6 play a key role in DMVs formation by inserting their hydrophobic transmembrane domain into ER. Further after replication of genomic and subgenomic RNA in RTC complex start translation of accessory proteins, structural (S, E, M proteins), and nonstructural proteins.

In the third step assembly of virion takes place. After the synthesis of these proteins, they are inserted into the endoplasmic reticulum, then move through the secretory pathway (ER-Golgi intermediate compartment [80, 81]. In this compartment, the viral genome is encapsulated by N protein forming the mature virion containing vesicles [82]. Further, virions packed in the vesicle are carried to the cell surface and delivered by membrane fusion and exocytosis. How transportation of virion happens exactly, not clear yet. Either it happens through large cargo from Golgi or virus follow different, novel exit pathway.

Cellular tropism

Both SARS-CoV and SARS-CoV-2 known to use human ACE2 receptor to take entry inside the cell [83]. SARS-CoV-2 mainly affects respiratory tract however there are several evidences that show broader cell tropism. Clinical manifestations of SARS-CoV-2 have been well defined and genome of SARS-CoV-2 is fully sequenced. However, much of the cellular tropism and its manifestation is still unclear and limited data on tissue and cellular tropism are available as of now. ACE2 receptors expression was significantly seen in alveolar, type II epithelial cells, heart, kidney, brain and gastrointestinal tract (especially in small and large intestines). The single cell RNA sequencing studies showed the presence of ACE2 mRNA in different cells of various organs such as lung epithelial cells, myocytes, kidney tubular cells,

oesophageal epithelial, urothelial cells [84–86]. Greater binding affinity with ACE2 might facilitate virus entry into pulmonary cells leading to higher transmission among people through various direct and indirect contacts with the patients [44]. The robust replicative property of coronavirus in bronchial as well as alveolar epithelium also describes the higher transmissibility of SARS-CoV-2 as compared to other CoVs. SARS-CoV-2 and SARS-CoV have shown significant replication in various cell lines that manifest their abilities to cause lower respiratory tract infection. Reports have shown replication competence and cellular tropism of SARS-CoV-2 in respiratory tract and extra pulmonary cells. SARS-CoV shown significant replication levels in both Calu3 (pulmonary cells) and Caco2 (intestinal cell) which indicated lower respiratory tract and gastrointestinal infection in COVID-19 patients [87].

Cardiovascular system

Cardiovascular manifestations are also one of the prominent consequences due to SARS-CoV-2 infection. This includes various cardiac injuries, stroke, coronary arterial ischemia, pulmonary embolism, arterial thrombosis etc. [88]. In a cohort study consisting of 2 groups (29 patients) infected with SARS-CoV-2, 30-fold increase in Kawasaki like disease were observed. [89] SARS-CoV-2 infection seems to be correlated with higher incidences of cardiac dysfunction and macrophage activation syndrome. [89].

Endothelial cell

Recent studies shown viral infection and inflammation in endothelial cell in COVID-19 infected patient due to presence of same ACE2 receptor on the surface of endothelial cells. Other than this, endothelial dysfunction has also been seen because of the recruitment of different immune cells by various direct and indirect infection caused by SARS-CoV-2, which is associated with cell death and multiple organ failure. [90].

Gastrointestinal tract and liver

Evidence from several studies indicated that coronavirus has a tropism to the gastrointestinal tract due to the presence of ACE2 receptor. Different cohort studies showed diarrhoea vomiting and other gastrointestinal problems [91–96]. Liver injury was also reported in the blood test reports of COVID-19 patients [97]. Elevated levels of alanine aminotransferase (ALT) and aspartate aminotransferase (AST) were also detected in cohort studies of infected patients [91, 92]. There was abnormal elevation of bilirubin during the infection. However, there was no severe damage observed in liver function, but the patients having severe viral infection

seems to have higher level of liver injury. Similar infection of colorectal carcinoma epithelial cell line shown replication of virus in gastrointestinal tract that hints possibility of oral-faecal transmission. These multiple routes of transmission might explain the rapid spread of COVID-19 worldwide.

Kidney

Cellular tropism for kidney was observed even in the patients who do not have any history of chronic renal disease. mRNA sequencing studies revealed that ACE2, TMPRSS, Cathepsin genes are present in kidney cells that facilitate the entry and infection of SARS-CoV-2 causing various kidney injuries [98]. Chronic kidney injuries are one of the strongest risk factors for COVID-19 related death [99, 100]. In the cohort study consisting post-mortem report of 63 patients, out of this SARS-CoV-2 RNA was found in 60% of the patients with kidney injuries. Renal tropism also shown to be associated with disease severity and kidney injury that leads to premature death [101].

Brain


SARS-CoV-2 also infects extra pulmonary tissue including CNS and PNS, mechanism of which is still not known. It is hypothesized that virus crosses the blood brain barrier to invade the brain that leads to various neurological manifestations including headache, dizziness, seizures, loss of consciousness. Reports have shown that SARS-CoV-2 can also cause viral encephalitis, meningitis, encephalopathy etc. Mao et. al [102] shown ischemic and haemorrhagic stroke as one of the neurological manifestations seen in 3% of infected patients.

Eyes

There are evidence showing conjunctival epithelium and conducting airways as potential portal of infection for SARS-CoV-2. Infection in conjunctiva suggests eye as additional route of infection [103].

Immunomodulation by SARS CoV-2

Innate immunity presents the first barrier for virus invasion. Pattern recognizing receptor (PRR) recognizes the molecular patterns associated with the virus and initiate a cascade of downstream signaling to release a burst of cytokines known as cytokine storm (Fig. 5). This include both Th₁ and Th₂ associated cytokines including IL1, IFN γ , IL10 etc. [104]. IL6 which is known to play an important antiviral role in case of influenza and herpes simplex virus (HSV) [105, 106] and its higher level is


Co-ordinator
IQAC, Shri Ram College,
Muzaffarnagar


Chairman
IQAC, Shri Ram College,
Muzaffarnagar

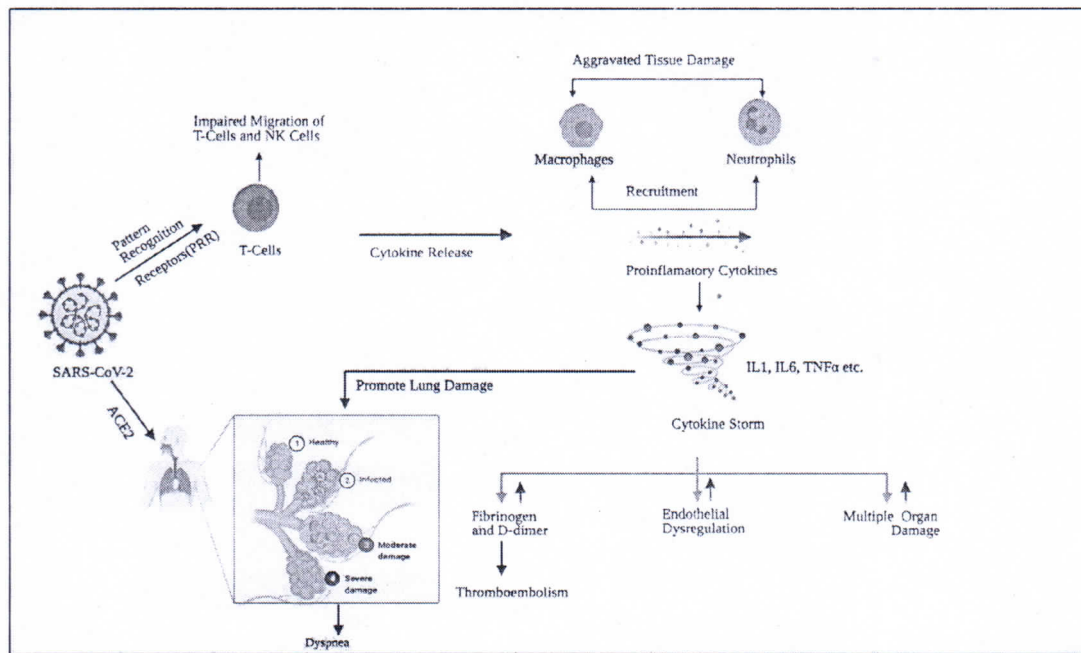


Fig. 5 Overview of immunological aspect of COVID-19 indicating the viral induced immune modulation in the infected host tissues. SARS-CoV-2 is recognised by the pattern recognising receptors by the T cells which in turn initiates a cascade of events particularly

cytokine storm, recruitment of inflammatory cells etc., ultimately resulting in multiple organ damage and the development of symptoms that are associated with the progression of COVID-19 disease

correlated with the severe progression of the disease and mortality in SARS-CoV and SARS-CoV-2. [107, 108] IL6 can be induced directly or indirectly by SARS. Studies found out that indirect stimulation happens when the virus bind to the toll like receptor 4 (TLR4) and induces IL6 expression through NF- κ B pathway [109]. Direct stimulation of IL6 occurs when structural protein (N protein) of SARS-CoV bind to the NF- κ B regulatory portion in the promoter region of IL6 [110]. IFN γ 1 pre-injection or early presence can limit or stop the virus associated damage with much more potency than in SARS-CoV [111]. Adaptive immune response in viral infected patient are drastically affected as helper T cells and cytotoxic T cells are significantly reduced in the peripheral circulation in moderate and severe cases of COVID-19 [112]. Number of CD8 memory T cells exceeds the CD4 memory T cells in the SARS-CoV survivor and virus specific T cells present in the blood for at least 6–11 years [113]. IFN γ and TNF α that are upregulated in the infected patient are responsible for the retention and binding of T cells to the epithelium in the lymphoid organs that may result in overall reduction in peripheral blood circulation. [114] Lavage fluid collected from the COVID-19 patients showed the clonal expansion of CD8 cells suggesting that T cell migration to the infected site that results in the overall lower peripheral counts. [115].

Immuno-pathogenesis

A study of 99 hospitalized patients in china showed that 12% had thrombocytopenia, 36% had elevated D dimer and proinflammatory cytokines, 5% show increase prothrombin and four others suffered from septic shock [116]. As already discussed, SARS-CoV-2 induced a burst of proinflammatory cytokines in the infected site. The higher level of these cytokines in the serum may be correlated with the lung lesion as these cytokines promoted the massive migration of immune cells to the infected site (Fig. 5). Also, type II alveolar cells of the lung express high level of ACE2 receptor, thus lung is one of the most susceptible organ to viral attack [117]. These lung lesion may be correlated with the dyspnea, a common symptom associated with COVID-19 [118]. Lung Natural killer (NK) cells doesn't possess the ACE2 receptor, exhibit CD16⁺KIR⁺ phenotype thus virus can't directly target these cells but studies found that after infection CD16⁺ NK cell significantly decreased in the peripheral blood suggesting defective migration or maturation process of NK cells [119, 120]. Thrombocytopenia is also normally observed symptom in the patients suffering from COVID-19. One hypothesis could be that virus may bind to CD13, a marker present on bone marrow cells and platelets and then induces apoptosis of the megakaryocytes thus resulting in decrease number of platelets [121]. Another hypothesis is

that SARS-CoV-2 bind the liver cells via ACE2 receptor and induces its damage. Liver cells produce thrombopoietin required for the differentiation and maturation of megakaryocytes in to the platelets [122, 123]. Also, lung damage induced by the proinflammatory cytokines reduces the capillary bed in the lung which may result in lower pulmonary recirculation and ultimate result is thrombocytopenia. [124, 125]. Further, increase in proinflammatory cytokine particularly IL6 induces fibrinogen and D dimer which may indicate a direct link between cytokine storm and procoagulation/thromboembolism in the virus infected persons [126–128].

Dysgensia (loss of taste) and Hyposmia (loss of smell) are an early indicator of SARS-CoV-2 infection [129]. Salivary gland and neural cells of olfactory epithelium express ACE2 receptors thus serves as a target of SARS-CoV-2. Infected salivary glands may produce less quantity and quality of saliva, thus resulting in dysgensia. [130] Damage to neuronal cells of olfactory epithelium, expressing high amount of ACE2 receptor may be a reason behind the partial loss of smell associated with the viral infection. [131].

Conclusion and future direction

This short review provides brief overview of available information of SARS-COV-2 origin, infectivity, biology, brief molecular insight of disease pathogenesis and progression. It also includes concise description of peculiar mutations, genome organization, cell tropism and immunomodulation/immunopathogenesis caused by SARS-CoV-2. Current pandemic caused by SARS-CoV-2 is the deadliest pandemic of twenty first century that took whole world on storm. Despite of our best effort and frenetic search of therapeutic we are not able to find the cure of COVID-19 even after more than one year since outbreak. Since last century we have witnessed several virus outbreaks i.e., Swine Flu, Ebola, Zika and so on. Even after much efforts pathogenic virus outbreaks keep happening and huge scientific advancement is not enough to combat such pandemics. The disease keeps spreading and taking toll on lives and economy despite of huge efforts and there are emergence of second and third wave across the globe. Researchers are unfolding mysteries around corona virus every day in all dimensions i.e., infectivity, clinical manifestation, drug trials and failures and vaccine development. Coronaviruses emergence is very rapid, repetitive and unpredictable. However, disease pathogenesis and involvement of several human receptors/proteins such ACE2, Cathepsine, and viral protein such as PLpro, CLpro and other accessory protein involved in disease progression are explored well now and can provides better insight for screening of new lead molecules for antiviral drug development. But, we need integrated approach involving


computational biology, genome analysis, immunology, proteomics studies, and systems biology along with various animal models for in depth information of disease progression and manifestation. To be better prepared to mitigate this kind of pandemic in future, it is very necessary to have multidisciplinary international consortium including virologist, molecular biologist, pathophysiologist, chemist, statistician and clinician. Considering the threat imposed by SARS-CoV-2, there is dire need to take virus research at deeper level for better understanding of pathogenesis from molecular to clinical level and to develop the advance therapeutic strategies to tackle COVID-19 like infection in future.

Current outbreak not only necessitates development of the broad spectrum antiviral drug but also the more robust, sustainable and responsive global public healthcare preparedness than ever. SARS-CoV-2 is far more infectious and widespread than earlier CoVs. There are challenges not only associated with virus but with patients as it imposes several issues like wide range of symptoms, severity and clinical manifestations. The disease need to be understood on various parameters such as heterogeneity in infected population, genetic makeup, co-morbidity/pre-existing medication for clear and comprehensive understanding for effective treatment. Immune-triggered response are worsening the treatment outcome and hampering the disease understanding. Drug repurposing has surfaced as life and time saver, cost effective alternative during COVID-19 pandemic. Currently, repurposed drugs are used to treat critical patients. However, there are challenges associated with drug repurposing such as dose optimization and dose associated toxicity that need to be addressed carefully. Virus affect the host immune response as well as organ function and repurposed drug can cause adverse pharmacological effect on ailing patients. Another important aspect which should be taken into consideration while using repurposed is pharmacogenomics which is overlooked due to extenuating situation to treat the critical patients. Pharmacogenomics is key parameter to establish for long term efficacy and safety of the drugs.

More so, zoonotic origin virus and pathogens outbreaks are inevitable and likely to continue in future so concerted and cohesive efforts considering all aspect are required to minimise the health care burden and death toll in future.

Acknowledgements We would like to thank Director, Institute of Nuclear Medicine and Applied Sciences (INMAS), for his continuous support. This work was funded by Defence Research Development Organization, India, Project No. S&T/18-19/INM-323. Images are created using Biorender.com

Authors Contribution The named two authors with equal contribution participated equally in designing the study, writing, and editing of the manuscript.


Co-ordinator
IQAC, Shri Ram College,
Muzaffarnagar


Chairman
IQAC, Shri Ram College,
Muzaffarnagar

Compliance with ethical standards

Conflict of interest The authors declare no competing interests.

References

- Gorbalenya AE, Baker SC, Baric RS, de Groot RJ, Drosten C, Gulyaeva AA, Haagmans BL, Lauber C, Leontovich AM, Neuman BW, Penzar D, Perlman S, Poon Samborskiy Sidorov Sola Ziebuhr LLMDIAIJ (2020) The species severe acute respiratory syndrome related coronavirus: classifying 2019-nCoV and naming it SARS-CoV-2. *Nat Microbiol* 5:536–544
- Krishnan A, Hamilton JP, Alqahtani SA, Woreta TA (2021) COVID-19: an overview and a clinical update. *World J Clin Cases* 9(1):8–23
- McGill AR, Kahlil R, Dutta R, Green R, Howell M, Mohapatra S, Mohapatra SS (2021) SARS-CoV-2 immuno-pathogenesis and potential for diverse vaccines and therapies: opportunities and challenges. *Infect Disease Rep* 13(1):102–125
- Tang Q, Song Y, Shi M, Cheng Y, Zhang W, Xia XQ (2015) Inferring the hosts of corona-virus using dual statistical models based on nucleotide composition. *Sci Rep* 5:17155
- Samavati L, Uhal BD (2020) ACE2, much more than just a receptor for SARS-COV-2. *Front Cell Infect Microbiol* 10:317
- Su S, Wong G, Shi W, Liu J, Lai AC, Zhou J, Liu W, Bi Y, Gao GF (2016) Epidemiology, genetic recombination, and pathogenesis of coronaviruses. *Trends Microbiol* 24(6):490–502
- Zhu N, Zhang D, Wang W, Li X, Yang B, Song J, Zhao X, Huang B, Shi W, Lu R, Niu P, Zhan F (2020) A novel coronavirus from patients with pneumonia in China, 2019. *New Engl J Med*. <https://doi.org/10.1056/NEJMoa2001017>
- Holshue ML, DeBolt C, Lindquist S, Lofy KH, Wiesman J, Bruce H, Spitters C, Ericson K, Wilkerson S, Tural A, Diaz G, Cohn A, Fox L, Patel A, Gerber SI, Kim L, Tong S, Lu X, Lindstrom S, Pallansch MA, Weldon WC, Biggs HM, Uyeki TM, Pillai SK, Washington State 2019-nCoV Case Investigation Team (2020) First Case of 2019 novel coronavirus in the United States. *New Engl J Med* 382(10):929–936
- Rothe C, Schunk M, Sothmann P, Bretzel G, Froeschl G, Wallrauch C, Zimmer T, Thiel V, Janke C, Guggemos W, Seilmaier M, Drosten C, Vollmar P, Zwirgmaier K, Zange S, Wölfel R, Hoelscher M (2020) Transmission of 2019-nCoV infection from an asymptomatic contact in Germany. *N Engl J Med* 382(10):970–971
- Li Q, Guan X, Wu P, Wang X, Zhou L, Tong Y, Ren R, Leung K, Lau E, Wong JY, Xing X, Xiang N, Wu Y, Li C, Chen Q, Li D, Liu T, Zhao J, Liu M, Tu W, Chen C, Jin L, Yang R, Wang Q, Zhou S, Wang R, Liu H, Luo Y, Liu Y, Shao G, Li H, Tao Z, Yang Y, Deng Z, Shi G, Lam TT, Wu JT, Gao GF, Cowling BJ, Yang B, Leung GM, Feng Z (2020) Early transmission dynamics in wuhan, china, of novel coronavirus-infected pneumonia. *N Engl J Med* 382(13):1199–1207
- Zhu N, Zhang D, Wang W, Li X, Yang B, Song J, Zhao X, Huang B, Shi W, Lu R, Niu P, Zhan F, Ma X, Wang D, Xu W, Wu G, Gao GF, Tan W, for the China Novel Coronavirus Investigating and Research Team (2020) A novel coronavirus from patients with pneumonia in China, 2019. *New Engl J Med*. <https://doi.org/10.1056/NEJMoa2001017>
- Ren LL, Wang YM, Wu ZQ, Xiang ZC, Guo L, Xu T, Jiang YZ, Xiong Y, Li YJ, Li XW, Li H, Fan GH, Gu XY, Xiao Y, Gao H, Xu JY, Yang F, Wang XM, Wu C, Chen L, Liu YW, Liu B, Yang J, Wang XR, Dong J, Li L, Huang CL, Zhao JP, Hu Y, Cheng ZS, Liu LL, Qian ZH, Qin C, Jin Q, Cao B, Wang JW (2020) Identification of a novel coronavirus causing severe pneumonia in human: a descriptive study. *Chin Med J* 133(9):1015–1024
- Liu K, Fang YY, Deng Y, Liu W, Wang MF, Ma JP, Xiao W, Wang YN, Zhong MH, Li CH, Li GC, Liu HG (2020) Clinical characteristics of novel coronavirus cases in tertiary hospitals in Hubei Province. *Chin Med J*. <https://doi.org/10.1097/CM9.0000000000000744>
- Wang D, Hu B, Hu C, Zhu F, Liu X, Zhang J, Wang B, Xiang H, Cheng Z, Xiong Y, Zhao Y, Li Y, Wang X, Peng Z (2020) Clinical characteristics of 138 hospitalized patients with 2019 novel coronavirus-infected pneumonia in Wuhan China. *JAMA* 323(11):1061–1069. <https://doi.org/10.1001/jama.2020.1585>
- Wu Z, McGoogan JM (2020) Characteristics of and important lessons from the coronavirus disease 2019 (COVID-19) outbreak in China: summary of a report of 72,314 cases from the Chinese Center for Disease Control and Prevention. *JAMA* 323(13):1239–1242
- Wenham C, Smith J, Morgan R (2020) COVID-19: the gendered impacts of the outbreak. *Lancet*. [https://doi.org/10.1016/S0140-6736\(20\)30526-2](https://doi.org/10.1016/S0140-6736(20)30526-2)
- Jin JM, Bai P, He W, Wu F, Liu XF, Han DM, Liu S, Yang JK (2020) Gender differences in patients with COVID-19: focus on severity and mortality. *Front Public Health* 8:152
- Li Q, Guan X, Wu P, Wang X, Zhou L, Tong Y, Ren R, Leung K, Lau E, Wong JY, Xing X, Xiang N, Wu Y, Li C, Chen Q, Li D, Liu T, Zhao J, Liu M, Tu W, Chen C, Jin L, Yang R, Wang Q, Zhou S, Wang R, Liu H, Luo Y, Liu Y, Shao G, Li H, Tao Z, Yang Y, Deng Z, Shi G, Lam TT, Wu JT, Gao GF, Cowling BJ, Yang B, Leung GM, Feng Z (2020) Early transmission dynamics in Wuhan, China, of novel coronavirus-infected pneumonia. *N Engl J Med* 382:1199–1207
- Yang Y, Lu Q, Liu M, Wang Y, Zhang A, Jalali N, Dean N, Longini I, Halloran ME, Xu B, Zhang X, Wang L, Liu W, Fang L (2020) Epidemiological and clinical features of the 2019 novel coronavirus outbreak in China. *MedRxiv*. <https://doi.org/10.1101/2020.02.10.20021675>
- Linton NM, Kobayashi T, Yang Y, Hayashi K, Akhmetzhanov AR, Jung SM, Yuan B, Kinoshita R, Nishiura H (2020) Incubation period and other epidemiological characteristics of 2019 novel coronavirus infections with right truncation: a statistical analysis of publicly available case data. *J Clin Med* 9(2):538
- Bi Q, Wu Y, Mei S, Ye C, Zou X, Zhang Z, Liu X, Wei L, True-love SA, Zhang T, Gao W, Cheng C, Tang X, Wu X, Wu Y, Sun B, Huang S, Sun Y, Zhang J, Ma T et al (2020) Epidemiology and transmission of COVID-19 in 391 cases and 1286 of their close contacts in Shenzhen, China: a retrospective cohort study. *Lancet Infect Dis* 20(8):911–919
- Guan WJ, Ni ZY, Hu Y, Liang WH, Ou CQ, He JX, Shan H, Lei CL, Hui DS, Du B, Li LJ, Zeng G, Yuen KY, Chen RC, Tang CL, Wang T, Chen PY, Xiang J, Li SY, Wang JL, Liang ZJ, Peng YX, Wei L, Liu Y, Hu YH, Peng P, Wang JM, Liu JY, Chen Z, Li G, Zheng ZJ, Ouyang SQ, Luo J, Ye CJ, Zhu SY, Zhong NS (2020) Clinical characteristics of 2019 novel coronavirus infection in China. *New Engl J Med*. <https://doi.org/10.1056/NEJMoa2002032>
- Huang C, Wang Y, Li X, Ren L, Zhao J, Hu Y, Zhang L, Fan G, Xu J, Gu X, Cheng Z, Yu T, Xia J, Wei Y, Wu W, Xie X, Yin W, Li H, Liu M, Xiao Y, Gao H, Guo L, Xie J, Wang G, Jiang R, Gao Z, Jin Z, Lin Q, Wang J, Cao B (2020) Clinical features of patients infected with 2019 novel coronavirus in Wuhan, China. *Lancet* 395(10223):497–506
- Zhu N, Zhang D, Wang W, Li X, Yang B, Song J, Zhao X, Huang B, Shi W, Lu R, Niu P, Zhan F, Ma X, Wang D, Xu W, Wu G, Gao GF, Tan W, China Novel Coronavirus Investigating and Research Team (2020) A novel coronavirus from patients with pneumonia in China, 2019. *New Engl J Med* 382(8):727–733

25. Zhou P, Yang XL, Wang XG, Hu B, Zhang L, Zhang W, Si HR, Zhu Y, Li B, Huang CL, Chen HD, Chen J, Luo Y, Guo H, Jiang RD, Liu MQ, Chen Y, Shen XR, Wang X, Zheng XS, Zhao K, Chen QJ, Deng F, Liu LL, Yan B, Zhan FX, Wang YY, Xiao G, Shi ZL (2020) Discovery of a novel coronavirus associated with the recent pneumonia outbreak in humans and its potential bat origin. *Nature*. <https://doi.org/10.1038/s41586-020-2012-7>
26. Sabir JS, Lam TTY, Ahmed MM, Li L, Shen Y, Abo-Aba SE, Qureshi MI, Zeid MA, Zhang Y, Khiyami MA, Alharbi NS, Hajrah NH, Sabir MJ, Mutwakil MH, Kabli SA, Alsulaimany FA, Obaid AY, Zhou B, Smith DK, Holmes EC, Zhu H, Guan Y (2016) Co-circulation of three camel coronavirus species and recombination of MERS-CoVs in Saudi Arabia. *Science* 351(6268):81–84
27. Lin XD, Wang W, Hao ZY, Wang ZX, Guo WP, Guan XQ, Wang MR, Wang HW, Zhou RH, Li MH, Tang GP, Wu J, Holmes EC, Zhang YZ (2017) Extensive diversity of coronaviruses in bats from China. *Virology* 507:1–10
28. Chen Y, Liu Q, Guo D (2020) Emerging coronaviruses: genome structure, replication, and pathogenesis. *J Med Virol* 92(4):418–423
29. Chan JF, Kok KH, Zhu Z, Chu H, To KK, Yuan S, Yuen K (2020) Genomic characterization of the 2019 novel human-pathogenic coronavirus isolated from a patient with atypical pneumonia after visiting Wuhan. *Emerg Microbes Infect* 9(1):221–236
30. Zhou P, Yang X, Wang X, Hu B, Zhang L, Zhang W, Si H, Zhu Y, Li B, Huang C, Chen H, Chen J, Luo Y, Guo H, Jiang R, Liu M, Chen Y, Shen X, Wang X, Zhang X, Zhao K, Chen Q, Deng F, Liu L, Yan B, Zhan F, Wang Y, Xiao G, Shi Z (2020) A pneumonia outbreak associated with a new coronavirus of probable bat origin. *Nature* 579:270–273
31. Mousavizadeh L, Ghasemi S (2020) Genotype and phenotype of COVID-19: their roles in pathogenesis. *J Microbiol Immunol Infect*. <https://doi.org/10.1016/j.jmii.2020.03.022>
32. Lokugamage KG, Hage A, Schindewolf C, Rajsbaum R, Menachery VD (2020) SARS-CoV-2 is sensitive to type I interferon pretreatment. *J Virol* 42:749
33. Khailany RA, Safdar M, Ozaslan M (2020) Genomic characterization of a novel SARS-CoV-2. *Gene Rep* 19:100682
34. Guo YR, Cao QD, Hong ZS, Tan YY, Chen SD, Jin HJ, Tan KS, Wang DY, Yan Y (2020) The origin, transmission and clinical therapies on coronavirus disease 2019 (COVID-19) outbreak—an update on the status. *Mil Med Res* 7(1):1–10
35. Wu A, Peng Y, Huang B, Ding X, Wang X, Niu P, Meng J, Zhu Z, Zhang Z, Wang J, Sheng J, Quan L, Xia Z, Tan W, Cheng G, Jiang T (2020) Genome composition and divergence of the novel coronavirus (2019-nCoV) originating in China. *Cell Host Microbe* 27:325
36. Wan Y, Shang J, Graham R, Baric RS, Li F (2020) Receptor recognition of novel corona virus from Wuhan: an analysis based on decade long structural studies of SARS coronavirus. *J Virol* 2020(4):1–5
37. Tai W, He L, Zhang X, Pu J, Voronin D, Jiang S, Zhou Y, Du L (2020) Characterization of the receptor-binding domain (RBD) of 2019 novel coronavirus: implication for development of RBD protein as a viral attachment inhibitor and vaccine. *Cell Mol Immunol* 17(6):613–620
38. Lu R, Zhao X, Li J, Niu P, Yang B, Wu H, Wang W, Song H, Huang B, Zhu N, Bi Y, Ma X, Zhan F, Wang L, Hu T, Zhou H, Hu Z, Zhou WZ, Zhao L, Chen J, Meng Y, Wang J, Lin Y, Yuan J, Xie Z, Ma J, Liu W, Wang D, Xu W, Holmes EC, Gao GF, Wu G, Chen W, Shi W, Tan W (2020) Genomic characterisation and epidemiology of 2019 novel coronavirus: implications for virus origins and receptor binding. *Lancet* 395(10224):565–574
39. Li F, Li WH, Farzan M, Harrison SC (2005) Structure of SARS coronavirus spike receptor-binding domain complexed with receptor. *Science* 309:1864–1868. <https://doi.org/10.1126/science.1116480>
40. Xia S, Zhu Y, Liu M, Lan Q, Xu W, Wu Y, Ying T, Liu S, Shi Z, Jiang S, Lu L (2020) Fusion mechanism of 2019-nCoV and fusion inhibitors targeting HR1 domain in spike protein. *Cell Mol Immunol* 17:1–3
41. Towler P, Staker B, Prasad SG, Menon S, Tang J, Parsons T, Ryan D, Fisher M, Williams D, Dales NA, Patane MA, Pantoliano MW (2004) ACE2 X-ray structures reveal a large hinge-bending motion important for inhibitor binding and catalysis. *J Biol Chem* 279(17):17996–18007
42. Wan Y, Shang J, Graham R, Baric RS, Li F (2020) Receptor recognition by the novel coronavirus from Wuhan: an analysis based on decade-long structural studies of SARS coronavirus. *J Virol*. <https://doi.org/10.1128/JVI.00127-20>
43. Walls AC, Park YJ, Tortorici MA, Wall A, McGuire AT, Veesler D (2020) Structure, function, and antigenicity of the SARS-CoV-2 spike glycoprotein. *Cell*. <https://doi.org/10.1016/j.cell.2020.02.058>
44. Wrapp D, Wang N, Corbett KS, Goldsmith JA, Hsieh CL, Abiona O, Graham BS, McLellan JS (2020) Cryo-EM structure of the 2019-nCoV spike in the prefusion conformation. *Science* 367(6483):1260–1263
45. Ortega JT, Serrano ML, Pujol FH, Rangel HR (2020) Role of changes in SARS-CoV-2 spike protein in the interaction with the human ACE2 receptor: an in silico analysis. *EXCLI J* 19:410–417
46. Wang K, Chen W, Zhou Y, Lian J, Zhang Z, Du P, Gong L, Zhang Y, Cui H, Geng J, Wang B, Sun X, Wang C, Yang X, Lin P, Deng Y, Wei D, Yang X, Zhu Y, Zhang K, Zheng Z, Miao J, Guo T, Shi Y, Zhang J, Fu L, Wang Q, Bian H, Zhu P, Chen Z (2020) SARS-CoV-2 invades host cells via a novel route: CD147-spike protein. *Signal Transduct Target Ther*. <https://doi.org/10.1038/s41392-020-00426-x>
47. Guo JP, Petric M, Campbell W, McGeer PL (2004) SARS corona virus peptides recognized by antibodies in the sera of convalescent cases. *Virology* 324(2):251–256
48. Yao HP, Lu X, Chen Q, Xu K, Chen Y, Cheng L, Liu F, Wu Z, Wu H, Jin C, Zheng M, Wu N, Jiang C, Li L (2020) Patient-derived mutations impact pathogenicity of SARS-CoV-2. *CELL-D-20-01124*. SSRN Electron J. <https://doi.org/10.2139/ssrn.3578153>
49. Andersen KG, Rambaut A, Lipkin WI, Holmes EC, Garry RF (2020) The proximal origin of SARS-CoV-2. *Nat Med* 26(4):450–452
50. Klenk HD, Garten W (1994) Host cell proteases controlling virus pathogenicity. *Trends Microbiol* 2(2):39–43
51. Zhang T, Wu Q, Zhang Z (2020) Probable pangolin origin of SARS-CoV-2 associated with the COVID-19 outbreak. *Curr Biol*. <https://doi.org/10.1016/j.cub.2020.03.063>
52. Watanabe Y, Allen JD, Wrapp D, McLellan JS, Crispin M (2020) Site-specific glycan analysis of the SARS-CoV-2 spike. *Science*. <https://doi.org/10.1126/science.abb9983>
53. Watanabe Y, Berndsen ZT, Raghvani J, Seabright GE, Allen JD, Pybus OG, McLellan JS, Wilson IA, Bowden TA, Ward AB, Crispin M (2020) Vulnerabilities in coronavirus glycan shields despite extensive glycosylation. *Nat Commun* 11(1):2688
54. Walls AC, Park YJ, Tortorici MA, Wall A, McGuire AT, Veesler D (2020) Structure, function, and antigenicity of the SARS-CoV-2 spike glycoprotein. *Cell* 181(2):281–292
55. Zhou P, Yang X, Wang XG, Hu B, Zhang L, Zhang W, Si HR, Zhu Y, Li B, Huang CL, Chen HD, Chen J, Luo Y, Guo H, Jiang RD, Liu MQ, Chen Y, Shen XR, Wang X, Zheng XS, Zhao K, Chen QJ, Den GF, Liu LL, Yan B, Zhan FX, Wang YY, Xiao GF, Shi ZL (2020) A pneumonia outbreak associated with a new coronavirus of probable bat origin. *Nature* 579(7798):270–273


Co-ordinator
IQAC, Shri Ram College,
Muzaffarnagar


Chairman
IQAC, Shri Ram College,
Muzaffarnagar

56. Bosch BJ, Van der Zee R, De Haan CA, Rottier PJM (2003) The coronavirus spike protein is a class I virus fusion protein: structural and functional characterization of the fusion core complex. *J Virol* 77(16):8801–8811
57. Tortorici MA, Walls AC, Lang Y, Wang C, Li Z, Koerhuis D, Boons GJ, Bosch BJ, Rey FA, Groot RJ, Veesler D (2019) Structural basis for human coronavirus attachment to sialic acid receptors. *Nat Struct Mol Biol* 26(6):481–489
58. Burkard C, Verheije MH, Wicht O, van Kasteren SI, van Kuppeveld FJ, Haagmans BL, Pelkmans L, Rottier PJ, Bosch BJ, de Haan CA (2014) Coronavirus cell entry occurs through the endo-/lysosomal pathway in a proteolysis-dependent manner. *PLoS Pathog* 10(11):e1004502
59. Kirchdoerfer RN, Cottrell CA, Wang N, Pallesen J, Yassine HM, Turner HL, Corbett KS, Graham BS, McLellan JS, Ward AB (2016) Pre-fusion structure of a human coronavirus spike protein. *Nature* 531(7592):118–121
60. Millet JK, Whittaker GR (2014) Host cell entry of Middle East respiratory syndrome coronavirus after two-step, furin-mediated activation of the spike protein. *Proc Natl Acad Sci USA* 111(42):15214–15219
61. Park JE, Li K, Barlan A, Fehr AR, Perlman S, McCray PB, Gallagher T (2016) Proteolytic processing of Middle East respiratory syndrome coronavirus spikes expands virus tropism. *Proc Natl Acad Sci USA* 113(43):12262–12267
62. Walls AC, Tortorici MA, Bosch BJ, Frenz B, Rottier PJ, DiMaio F, Rey FA, Veesler D (2016) Cryo-electron microscopy structure of a coronavirus spike glycoprotein trimer. *Nature* 531(7592):114–117
63. Madu IG, Roth SL, Belouzard S, Whittaker GR (2009) Characterization of a highly conserved domain within the severe acute respiratory syndrome coronavirus spike protein S2 domain with characteristics of a viral fusion peptide. *J Virol* 83(15):7411–7421
64. Millet JK, Whittaker GR (2015) Host cell proteases: Critical determinants of coronavirus tropism and pathogenesis. *Virus Res* 202:120–134
65. Belouzard S, Chu VC, Whittaker GR (2009) Activation of the SARS coronavirus spike protein via sequential proteolytic cleavage at two distinct sites. *Proc Natl Acad Sci USA* 106(14):5871–5876
66. Heald-Sargent T, Gallagher T (2012) Ready, set, fuse! The coronavirus spike protein and acquisition of fusion competence. *Viruses* 4(4):557–580
67. Walls AC, Tortorici MA, Snijder J, Xiong X, Bosch BJ, Rey FA, Veesler D (2017) Tectonic conformational changes of a coronavirus spike glycoprotein promote membrane fusion. *Proc Natl Acad Sci USA* 114(42):11157–11162. <https://doi.org/10.1073/pnas.1708727114>
68. Bergmann CC, Lane TE, Stohlman SA (2006) Coronavirus infection of the central nervous system: host–virus stand-off. *Nat Rev Microbiol* 4(2):121–132
69. White JM, Delos SE, Brecher M, Schornberg K (2008) Structures and mechanisms of viral membrane fusion proteins: multiple variations on a common theme. *Crit Rev Biochem Mol Biol* 43(3):189–219
70. White JM, Whittaker GR (2016) Fusion of enveloped viruses in endosomes. *Traffic* 17(6):593–614
71. Hoffmann M, Kleine-Weber H, Schroeder S, Krüger N, Herrler T, Erichsen S, Schiergens TS, Herrler G, Wu NH, Nitsche A, Müller MA, Drosten C, Pöhlmann S (2020) SARS-CoV-2 cell entry depends on ACE2 and TMPRSS2 and is blocked by a clinically proven protease inhibitor. *Cell* 181(2):271–280.e8. <https://doi.org/10.1016/j.cell.2020.02.052>
72. Guillén J, Kinnunen PK, Villalain J (2008) Membrane insertion of the three main membranotropic sequences from SARS-CoV S2 glycoprotein. *Biochim Biophys Acta* 1778(12):2765–2774
73. Lentz BR, Malinin V, Haque ME, Evans K (2000) Protein machines and lipid assemblies: current views of cell membrane fusion. *Curr Opin Struct Biol* 10(5):607–615
74. Cui J, Li F, Shi ZL (2019) Origin and evolution of pathogenic coronaviruses. *Nat Rev Microbiol* 17:181–192
75. Sola I, Almazán F, Zúñiga S, Enjuanes L (2015) Continuous and discontinuous RNA synthesis in coronaviruses. *Annu Rev Virol* 2(1):265–288. <https://doi.org/10.1146/annurev-virol-100114-055218>
76. Alonso S, Izeta A, Sola I, Enjuanes L (2002) Transcription regulatory sequences and mRNA expression levels in the coronavirus transmissible gastroenteritis virus. *J Virol* 76(3):1293–1308
77. Zúñiga S, Sola I, Alonso S, Enjuanes L (2004) Sequence motifs involved in the regulation of discontinuous coronavirus subgenomic RNA synthesis. *J Virol* 78:980–994
78. Pasternak AO, van den Born E, Spaan WJ, Snijder EJ (2001) Sequence requirements for RNA strand transfer during nidovirus discontinuous subgenomic RNA synthesis. *EMBO J* 20:7220–7228
79. Knoops K, Kikkert M, Van Den Worm SH, Zevenhoven-Dobbe JC, Van Der Meer Y, Koster AJ, Mommaas AM, Snijder EJ (2008) SARS-coronavirus replication is supported by a reticulovesicular network of modified endoplasmic reticulum. *PLoS Biol* 6(9):e226
80. Krijnse-Locker J, Ericsson M, Rottier PJ, Griffiths G (1994) Characterization of the budding compartment of mouse hepatitis virus: evidence that transport from the RER to the Golgi complex requires only one vesicular transport step. *J Cell Biol* 124(1):55–70
81. Tooze J, Tooze S, Warren G (1984) Replication of coronavirus MHV-A59 in sac-cells: determination of the first site of budding of progeny virions. *Eur J Cell Biol* 33(2):281–293
82. de Haan CA, Rottier PJ (2005) Molecular interactions in the assembly of coronaviruses. *Adv Virus Res* 64:165–230
83. Zhou P, Yang XL, Wang XG, Hu B, Zhang L, Zhang W, Si HR, Zhu Y, Li B, Huang CL, Chen HD, Chen J, Luo Y, Guo H, Jiang RD, Liu MQ, Chen Y, Shen XR, Wang X, Zheng XS et al (2020) A pneumonia outbreak associated with a new coronavirus of probable bat origin. *Nature* 579(7798):270–273. <https://doi.org/10.1038/s41586-020-2012-7>
84. Hamming I, Timens W, Bulthuis ML, Leij AT, Navis G, van Goor H (2004) Tissue distribution of ACE2 protein, the functional receptor for SARS coronavirus. A first step in understanding SARS pathogenesis. *J Pathol* 203:631–637
85. Monteil V, Kwon H, Prado P, Hagelkruys A, Wimmer RA, Stahl M (2020) Inhibition of SARS-CoV-2 infections in engineered human tissues using clinical-grade soluble human ACE2. *Cell* 181:905–913
86. Guo J, Huang Z, Lin L, Lv JC (2019) Coronavirus disease 2019 (COVID-19) and cardiovascular disease: a viewpoint on the potential influence of angiotensin-converting enzyme inhibitors/angiotensin receptor blockers on onset and severity of severe acute respiratory syndrome coronavirus 2 infection. *J Am Heart Assoc* 2020:9
87. Chu H, Chan JF, Yuen TT, Shuai H, Yuan S, Wang Y, Hu B, Yip CC, Tsang JO, Huang X, Chai Y, Yang D, Hou Y, Chik KK, Zhang X, Fung AY, Tsoi HW, Cai JP, Chan WM, Ip JD et al (2020) Comparative tropism, replication kinetics, and cell damage profiling of SARS-CoV-2 and SARS-CoV with implications for clinical manifestations, transmissibility, and laboratory studies of COVID-19: an observational study. *Lancet Microbe* 1(1):e14–e23. [https://doi.org/10.1016/S2666-5247\(20\)30004-5](https://doi.org/10.1016/S2666-5247(20)30004-5)
88. Guo T, Fan Y, Chen M, Wu X, Zhang L, He T, Wang H, Wan J, Wang X, Lu Z (2020) Cardiovascular implications of fatal outcomes of patients with coronavirus disease 2019 (COVID-19).

- JAMA Cardiol 5(7):811–818. <https://doi.org/10.1001/jamacardio.2020.1017>
89. Verdoni L, Mazza A, Gervasoni A, Martelli L, Ruggeri M, Ciuffreda M, Bonanomi E, D'Antiga L (2020) An outbreak of severe Kawasaki-like disease at the Italian epicentre of the SARS-CoV-2 epidemic: an observational cohort study. *Lancet* 395(10239):1771–1778. [https://doi.org/10.1016/S0140-6736\(20\)31103-X](https://doi.org/10.1016/S0140-6736(20)31103-X)
 90. Varga Z, Flammer AJ, Steiger P, Haberecker M, Andermatt R, Zinkernagel AS, Mehra MR, Schuepbach RA, Ruschitzka F, Moch H (2020) Endothelial cell infection and endotheliitis in COVID-19. *Lancet* 395(10234):1417–1418. [https://doi.org/10.1016/S0140-6736\(20\)30937-5](https://doi.org/10.1016/S0140-6736(20)30937-5)
 91. Chen N, Zhou M, Dong X et al (2020) Epidemiological and clinical characteristics of 99 cases of 2019 novel coronavirus pneumonia in Wuhan, China: a descriptive study. *Lancet* 395:507–513
 92. Huang C, Wang Y, Li X et al (2020) Clinical features of patients infected with 2019 novel coronavirus in Wuhan, China. *Lancet* 395:497–506
 93. Liu K, Fang YY, Deng Y et al (2020) Clinical characteristics of novel coronavirus cases in tertiary hospitals in Hubei Province. *Chin Med J (Engl)*. <https://doi.org/10.1097/CM9.0000000000000744>
 94. Xu XW, Wu XX, Jiang XG et al (2020) Clinical findings in a group of patients infected with the 2019 novel coronavirus (SARS-CoV-2) outside of Wuhan, China: retrospective case series. *BMJ* 368:m606
 95. Yang X, Yu Y, Xu J et al (2020) Clinical course and outcomes of critically ill patients with SARS-CoV-2 pneumonia in Wuhan, China: a single-centered, retrospective, observational study. *Lancet Respir Med*. [https://doi.org/10.1016/S2213-2600\(20\)30079-5](https://doi.org/10.1016/S2213-2600(20)30079-5)
 96. Zhou F, Yu T, Du R et al (2020) Clinical course and risk factors for mortality of adult inpatients with COVID-19 in Wuhan, China: a retrospective cohort study. *Lancet* 28:1054
 97. Guan WJ, Ni ZY, Hu Y et al (2020) Clinical characteristics of coronavirus disease 2019 in China. *N Engl J Med* 382:1708
 98. Pan XW, Xu D, Zhang H, Zhou W, Wang LH, Cui XG (2020) Identification of a potential mechanism of acute kidney injury during the COVID-19 outbreak: a study based on single-cell transcriptome analysis. *Intensive Care Med* 46(6):1114–1116. <https://doi.org/10.1007/s00134-020-06026-1>
 99. Yalameha B, Roshan B, Lakkakula VKS, Bhaskar ML (2020) Perspectives on the relationship of renal disease and coronavirus disease 2019. *J Nephropharmacol*. 9(2):e22
 100. Khouchlaa A, Bouyahya A (2020) COVID-19 nephropathy; probable mechanisms of kidney failure. *J Nephropathol*. 9:e35
 101. Braun F, Lütgehetmann M, Pfefferle S, Wong MN, Carsten A, Lindenmeyer MT, Nörz D, Heinrich F, Meißner K, Wichmann D, Kluge S, Gross O, Püeschel K, Schröder AS, Edler C, Aepfelbacher M, Puelles VG, Huber TB (2020) SARS-CoV-2 renal tropism associates with acute kidney injury. *Lancet* 396(10251):597–598
 102. Mao L, Jin H, Wang M, Hu Y, Chen S, He Q, Chang J, Hong C, Zhou Y, Wang D, Miao X, Li Y, Hu B (2020) Neurologic manifestations of hospitalized patients with coronavirus disease 2019 in Wuhan, China. *JAMA Neurol* 77(6):683–690
 103. Hui KPY, Cheung MC, Perera RAPM et al (2020) Tropism, replication competence, and innate immune responses of the coronavirus SARS-CoV-2 in human respiratory tract and conjunctiva: an analysis in ex-vivo and in-vitro cultures. *Lancet Respir Med* 8(7):687–695. [https://doi.org/10.1016/S2213-2600\(20\)30193-4](https://doi.org/10.1016/S2213-2600(20)30193-4)
 104. Huang C, Wang Y, Li X, Ren L, Zhao J, Hu Y, Zhang L, Fan G, Xu J, Gu X, Cheng Z, Yu T, Xia J, Wei Y, Wu W, Xie X, Yin W, Li H, Liu M, Xiao Y, Gao H, Guo L, Xie J, Wang G, Jiang R, Gao Z, Jin Q, Wang J, Cao B (2020) Clinical features of patients infected with 2019 novel coronavirus in Wuhan, China. *Lancet* 395(10223):497–506. [https://doi.org/10.1016/S0140-6736\(20\)30183-5](https://doi.org/10.1016/S0140-6736(20)30183-5) (PMID: 31986264)
 105. Dienz O, Rud JG, Eaton SM, Lanthier PA, Burg E, Drew A, Bunn J, Suratt BT, Haynes L, Rincon M (2012) Essential role of IL-6 in protection against H1N1 influenza virus by promoting neutrophil survival in the lung. *Mucosal Immunol* 5(3):258–266. <https://doi.org/10.1038/mi.2012.2> (PMID: 22294047)
 106. Murphy EA, Davis JM, Brown AS, Carmichael MD, Ghaffar A, Mayer EP (2008) Effect of IL-6 deficiency on susceptibility to HSV-1 respiratory infection and intrinsic macrophage antiviral resistance. *J Interferon Cytokine Res* 28(10):589–595
 107. Day CW, Baric R, Cai SX, Frieman M, Kumaki Y, Morrey JD et al (2009) A new mouse-adapted strain of SARS-CoV as a lethal model for evaluating antiviral agents in vitro and in vivo. *Virology* 395(2):210–222. <https://doi.org/10.1016/j.virol.2009.09.023>
 108. Zhou F, Yu T, Du R, Fan G, Liu Y, Liu Z, Xiang J, Wang Y, Song B, Gu X, Guan L, Wei Y, Li H, Wu X, Xu J, Tu S, Zhang Y, Chen H, Cao B (2020) Clinical course and risk factors for mortality of adult inpatients with COVID-19 in Wuhan, China: a retrospective cohort study. *Lancet* 395(10229):1054–1062. [https://doi.org/10.1016/S0140-6736\(20\)30566-3](https://doi.org/10.1016/S0140-6736(20)30566-3) (PMID: 32171076)
 109. Nyati KK, Masuda K, Zaman MM et al (2017) TLR4-induced NF-κB and MAPK signaling regulate the IL-6 mRNA stabilizing protein Arid5a. *Nucleic Acids Res* 45(5):2687–2703. <https://doi.org/10.1093/nar/gkx064>
 110. Zhang X, Wu K, Wang D et al (2007) Nucleocapsid protein of SARS-CoV activates interleukin-6 expression through cellular transcription factor NF-κB. *Virology* 365(2):324–335. <https://doi.org/10.1016/j.virol.2007.04.009>
 111. Blanco-Melo D, Nilsson-Payant BE, Liu WC, Uhl S, Hoagland D, Moller R, Jordan TX, Oishi K, Panis M, Sachs D, Wang TT, Schwartz RE, Lim JK, Albrecht RA, TenOever BR (2020) Imbalanced host response to SARS-CoV-2 drives development of COVID-19. *Cell* 181(5):1036–1045.e9
 112. Chen G, Wu D, Guo W, Cao Y, Huang D, Wang H, Wang T, Zhang X, Chen H, Yu H, Zhang X, Zhang M, Wu S, Song J, Chen T, Han M, Li S, Luo X, Zhao J, Ning Q (2020) Clinical and immunological features of severe and moderate coronavirus disease 2019. *J Clin Invest* 130(5):2620–2629
 113. Ng OW, Chia A, Tan AT, Jadi RS, Leong HN, Bertoletti A, Tan YJ (2016) Memory T cell responses targeting the SARS coronavirus persist up to 11 years post-infection. *Vaccine* 34(17):2008–2014. <https://doi.org/10.1016/j.vaccine.2016.02.063> (PMID: 26954467)
 114. Kamphuis E, Junt T, Waibler Z, Forster R, Kalinke U (2006) Type I interferons directly regulate lymphocyte recirculation and cause transient blood lymphopenia. *Blood* 108:3253–3261
 115. Liao M, Liu Y, Yuan J, Wen Y, Xu G, Zhao J, Cheng L, Li J, Wang X, Wang F, Liu L, Amit I, Zhang S, Zhang Z (2020) Single-cell landscape of bronchoalveolar immune cells in patients with COVID-19. *Nat Med* 26(6):842–844
 116. Chen N, Zhou M, Dong X, Qu J, Gong F, Han Y, Qiu Y, Wang J, Liu Y, Wei Y, Xia J, Yu T, Zhang X, Zhang L (2020) Epidemiological and clinical characteristics of 99 cases of 2019 novel coronavirus pneumonia in Wuhan, China: a descriptive study. *Lancet* 395(10223):507–513
 117. Lu R, Zhao X, Li J, Niu P, Yang B, Wu H, Wang W, Song H, Huang B, Zhu N, Bi Y, Ma X, Zhan F, Wang L, Hu T, Zhou H, Hu Z, Zhou W, Zhao L, Chen J, Meng Y, Wang J, Lin Y, Yuan J, Xie Z, Ma J, Liu WJ, Wang D, Xu W, Holmes EC, Gao GF, Wu G, Chen W, Shi W, Tan W (2020) Genomic characterisation and epidemiology of 2019 novel coronavirus: implications for virus origins and receptor binding. *Lancet* 395(10224):565–574
 118. Xu XW, Wu XX, Jiang XG, Xu KJ, Ying LJ, Ma CL, Li SB, Wang HY, Zhang S, Gao HN, Sheng JF, Cai HL, Qiu YQ, Li LJ

- (2020) Clinical findings in a group of patients infected with the 2019 novel coronavirus (SARS-Cov-2) outside of Wuhan, China: retrospective case series. *BMJ* 368:m606
119. National Research Project for SARS, Beijing Group (2004) The involvement of natural killer cells in the pathogenesis of severe acute respiratory syndrome. *Am J Clin Pathol* 121(4):507–511
 120. Wang F, Nie J, Wang H, Zhao Q, Xiong Y, Deng L, Song S, Ma Z, Mo P, Zhang Y (2020) Characteristics of peripheral lymphocyte subset alteration in COVID-19 pneumonia. *J Infect Dis* 221(11):1762–1769
 121. Yeager CL, Ashmun RA, Williams RK, Cardellichio CB, Shapiro LH, Look AT, Holmes KV (1992) Human aminopeptidase N is a receptor for human coronavirus 229E. *Nature* 357(6377):420–422
 122. Kaushansky K (2008) Historical review: megakaryopoiesis and thrombopoiesis. *Blood* 111(3):981–986
 123. Karagiannis P, Eto K (2015) Manipulating megakaryocytes to manufacture platelets ex vivo. *J Thromb Haemost* 13(Suppl 1):S47–S53
 124. Niinikoski J, Goldstein R, Linsey M, Hunt TK (1973) Effect of oxygen-induced lung damage on tissue oxygen supply. *Acta Chir Scand* 139(7):591–595
 125. Martin JF, Slater DN, Trowbridge EA (1983) Abnormal intrapulmonary platelet production: a possible cause of vascular and lung disease. *Lancet* 1(8328):793–796
 126. Levi M, Scully M (2018) How I treat disseminated intravascular coagulation. *Blood* 131(8):845–854. <https://doi.org/10.1182/blood-2017-10-804096>
 127. Ranucci M, Ballotta A, Di Dedda U, Bayshnikova E, Dei Poli M, Resta M, Falco M, Albano G, Menicanti L (2020) The procoagulant pattern of patients with COVID-19 acute respiratory distress syndrome. *J Thromb Haemost* 18(7):1747–1751
 128. Lippi G, Bonfanti L, Saccenti C, Cervellin G (2014) Causes of elevated D-dimer in patients admitted to a large urban emergency department. *Eur J Intern Med* 25(1):45–48
 129. Pierron D, Pereda-Loth V, Mantel M et al (2020) Smell and taste changes are early indicators of the COVID-19 pandemic and political decision effectiveness. *Nat Commun* 11:5152
 130. Butowt R, Bilinska K (2020) SARS-CoV-2: olfaction, brain infection, and the urgent need for clinical samples allowing earlier virus detection. *ACS Chem Neurosci* 11(9):1200–1203
 131. Wang WK, Chen SY, Liu IJ et al (2004) Detection of SARS-associated coronavirus in throat wash and saliva in early diagnosis. *Emerg Infect Dis* 10(7):1213–1219

Publisher's Note Springer Nature remains neutral with regard to jurisdictional claims in published maps and institutional affiliations.


Co-ordinator
IQAC, Shri Ram College,
Muzaffarnagar


Chairman
IQAC, Shri Ram College,
Muzaffarnagar